

# Atypical non-Basset particle dynamics due to hydrodynamic slip

Cite as: Phys. Fluids **32**, 097109 (2020); <https://doi.org/10.1063/5.0021986>

Submitted: 16 July 2020 . Accepted: 08 September 2020 . Published Online: 23 September 2020

A. R. Premlata , and Hsien-Hung Wei (魏憲鴻) 



View Online



Export Citation



CrossMark

## ARTICLES YOU MAY BE INTERESTED IN

[Cole–Cole relation for long-chain branching from general rigid bead–rod theory](#)

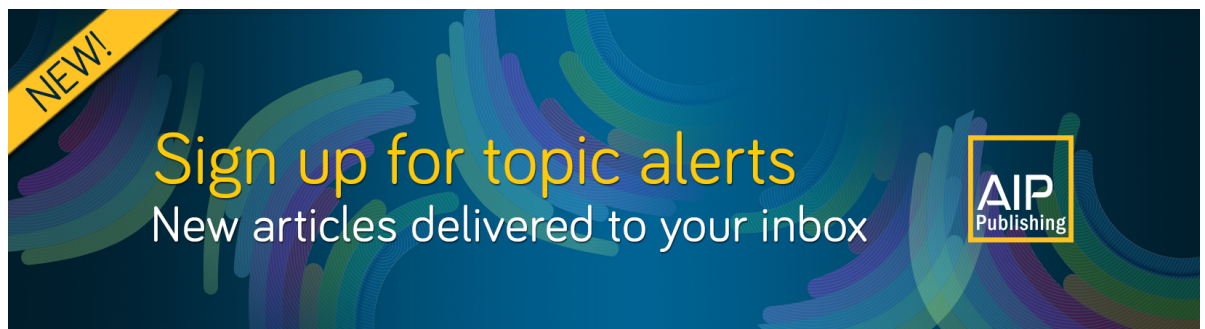
Physics of Fluids **32**, 093106 (2020); <https://doi.org/10.1063/5.0024402>

[Rheology of a dilute suspension of deformable microswimmers](#)

Physics of Fluids **32**, 071902 (2020); <https://doi.org/10.1063/5.0010558>


[Inertial migration of spherical particles in channel flow of power law fluids](#)

Physics of Fluids **32**, 083103 (2020); <https://doi.org/10.1063/5.0013725>



**NEW!**

Sign up for topic alerts  
New articles delivered to your inbox



# Atypical non-Basset particle dynamics due to hydrodynamic slip

Cite as: Phys. Fluids 32, 097109 (2020); doi: 10.1063/5.0021986

Submitted: 16 July 2020 • Accepted: 8 September 2020 •

Published Online: 23 September 2020



A. R. Premrata and Hsien-Hung Wei (魏憲鴻) <sup>a)</sup>

## AFFILIATIONS

Department of Chemical Engineering, National Cheng Kung University, Tainan 701, Taiwan

<sup>a)</sup> Author to whom correspondence should be addressed: [hhwei@mail.ncku.edu.tw](mailto:hhwei@mail.ncku.edu.tw)

## ABSTRACT

Surface slip does not simply reduce drag but strongly influences the behavior of unsteady particle motion. In this work, we revise the Maxey–Riley type equations in conjunction with the modified Faxen laws, showing that slip particles in unsteady motion, even if the amounts of slip are minuscule, can behave markedly different than no-slip particles due to the non-Basset history force and torque. The non-Basset memory kernels here are identified to be of Mittag–Leffler type but featured with the unique slip–stick transition that exists only for partial slip particles but not for full slip bubbles. The impacts especially manifest in the short time regime, illustrated with transient sedimentation, translational response to a suddenly applied stream, and angular response to a torque impulse. In these examples, the translational and angular velocities of a slip sphere are found to vary with time in different powers compared to those of single no-slip spheres. Dynamic distinctions to a spherical bubble can be best revealed by the asynchronous spinning of a slip sphere in an oscillatory vortical flow, showing that an additional inertia torque can arise from slip to give rise to a non-monotonic spinning response when the sphere is lighter than the surrounding fluid. As these non-Basset particle dynamics are rather atypically sensitive to the slip length, the impacts could be crucial to aerosol suspensions and inertial swimming of active hydrophobic particles where slip effects can no longer be negligible. The features might also have potential uses for achieving efficient hydrodynamic sorting of slip particles.

Published under license by AIP Publishing. <https://doi.org/10.1063/5.0021986>

## I. INTRODUCTION

Unsteady hydrodynamics plays an important role in many particulate systems. The impacts can be seen in swimming of self-propelled microorganisms,<sup>1,2</sup> acoustically or magnetically driven particle motion,<sup>3,4</sup> aerosol transport,<sup>5</sup> inertial particle trapping,<sup>6</sup> and particle clustering in turbulence.<sup>7</sup> For a spherical particle (of radius  $a$ ) advected by an ambient flow field  $\mathbf{u}^\infty$  in a viscous fluid (of density  $\rho$  and viscosity  $\mu$ ), its motion when migrating at a velocity  $\mathbf{U}$  is commonly described by the following classical Maxey–Riley equation:<sup>8–12</sup>

$$m_p \frac{d\mathbf{U}}{dt} = F_{ex} + F_{FI} + F_{AM} + F_S + F_H, \quad (1a)$$

$$F_{FI} = m_f \left. \frac{D\mathbf{u}^\infty}{Dt} \right|_{X(t)}, \quad (1b)$$

$$F_{AM} = \frac{-m_f}{2} \left[ \frac{d\mathbf{U}}{dt} - \frac{d}{dt} \left( 1 + \frac{a^2}{10} \nabla^2 \right) \mathbf{u}^\infty \right]_{X(t)}, \quad (1c)$$

$$F_S = -6\pi\mu a \mathbf{W}, \quad (1d)$$

$$F_H = -6\pi\mu a \left\{ \int_0^t G_B(t-t') \frac{d\mathbf{W}}{dt'} dt' + G_B(t) \mathbf{W}(0^-) \right\}, \quad (1e)$$

$$\mathbf{W}(t) = \mathbf{U}(t) - \left( 1 + \frac{a^2}{6} \nabla^2 \right) \mathbf{u}^\infty \Big|_{X(t)}, \quad (1f)$$

$$G_B(t) = \frac{1}{\sqrt{\pi}} \left( \frac{a^2/\nu}{t} \right)^{1/2}. \quad (1g)$$

Equation (1) is valid only when the particle Reynolds number is small based on the particle's velocity relative to that of the fluid. It is essentially the Basset–Boussinesq–Oseen equation<sup>13–15</sup> with the inclusion of finite-size effects reflected by additional Faxen corrections,  $a^2 \nabla^2 \mathbf{u}^\infty$ . In (1a)–(1c),  $m_p = (4\pi/3)\rho_p a^3$  is the mass of the particle (of density  $\rho_p$ ) positioned at  $X(t)$ ,  $m_f = (\rho/\rho_p)m_p$  is the fluid

mass displaced by the particle, and  $D/Dt$  is the substantial derivative. As revealed by Eq. (1), aside from the instantaneous Stokes drag  $F_S$ , the particle will further undergo three additional hydrodynamic forces to counteract the driving external force  $F_{ex}$ , the fluid inertial force  $F_{FI}$ , the added mass  $F_{AM}$ , and the history force  $F_H$ . Among these forces, the history force takes the form of a memory integral with the Basset kernel  $G_B$  to account for effects of vorticity diffusion during viscous relaxation in the time scale  $a^2/\nu$  (with  $\nu = \mu/\rho$  being the kinematic viscosity of the fluid). For this reason, this force has been shown to play an important role in particle dynamics.<sup>5,7,11,16–21</sup>

Notice that in the derivation of the Maxey–Riley equation (1), the no-slip boundary condition is assumed on the surface of a particle. In the situations involving aerosols and hydrophobic particles, however, a considerable amount of fluid slippage may exist on the surfaces of these particles. In this case, one may think that slip does nothing but drag reduction by merely modifying the coefficients in Eq. (1) without causing any qualitative changes in the particle motion. However, this is not true. The reason is that the memory kernel with slip, no matter how small the slip length is, will no longer take the no-slip Basset type-like Eq. (1g),<sup>22–24</sup> which may, in turn, change the features of unsteady particle motion qualitatively. Most of the existing studies have been devoted to resistance problems by looking at how the unsteady force and torque on a particle are modified by slip under prescribed particle motions.<sup>22–30</sup> However, much harder mobility problems, which aim to determine the non-Basset motion behavior of a slip particle in response to such force and torque, are still lacking, in noticeable contrast to extensive studies on the Basset dynamics of single no-slip particles under the Basset–Boussinesq–Oseen/Maxey–Riley paradigm. Given that a fraction of slip can change the memory kernel from Basset type to non-Basset type, how does a slip particle in unsteady motion behave compared to a no-slip particle? This is the main question we want to answer in this work.

We notice that non-Basset memory kernels can also happen to fluid particles whose surfaces are generally slipping.<sup>31,32</sup> There are a few reports on the transient motion responses of bubbles/full slipping particles and drops in the spherical shape.<sup>32–37</sup> However, on the non-Basset dynamics for slip particles, it is still waiting to be explored. A natural question is as follows: Would a slip particle in unsteady motion behave differently than a fluid particle?

Aside from the above issues that motivate this work, another incentive to look at the non-Basset particle dynamics arising from slip effects is the need of discriminating slip particles from no-slip or fluid particles hydrodynamically. This is essentially pertaining to how to sort slip particles experimentally. In practice, it is generally difficult to perform hydrodynamic sorting for slip particles under the steady Stokes flow condition. This is because the Stokes drag on a slip particle merely deviates up to 2/3 value of that on a no-slip particle. Compared to the drag on a bubble or drop, it is even harder to tell the difference because there is always slip on a fluid–fluid interface. If a particle is partially slip, especially when its slip length is much smaller than its size, it would be even unlikely to see any apparent difference in its motion compared to those of no-slip and fluid particles. Yet, in the unsteady situation, since these different types of particles have their own memory kernels, it seems possible that particle sorting can be made more effective in a dynamic manner, especially by utilizing differences in their unsteady motion responses

resulting from distinct history force characters. Therefore, to realize such dynamic particle sorting, it demands not only the knowledge of how a slip particle behaves dynamically but also how its motion differs compared to those of no-slip and fluid particles.

As non-Basset kernels are not limited to slip particles but also can occur to fluid particles, why those for slip particles are so special? To see this, it is, first of all, necessary to look at how a non-Basset kernel differs from the Basset kernel (1g). A non-Basset memory kernel typically involves a functional form,

$$\exp(\gamma t) \operatorname{erfc}((\gamma t)^{1/2}), \quad (2)$$

where  $\gamma$  measures the rate of the temporal attenuation of the kernel. Such a function is actually a special class of Mittag–Leffler functions,<sup>38</sup> and the memory kernels of this type frequently appear in the fractional Langevin equation for modeling anomalous diffusion.<sup>39</sup> Equation (2) reveals that it is finite as  $t \rightarrow 0$ , in contrast to the Basset kernel (1g) that diverges as  $t \rightarrow 0$ . This is the main difference between non-Basset and Basset kernels. For a fluid drop, it has been shown that its memory kernel constitutes an additional non-Basset kernel like (2) on top of a Basset kernel.<sup>31,32</sup> Hence, the memory kernel in this case is of mixed type and is singular at  $t = 0$ . It has to be the case since it guarantees that it reduces to the singular Basset kernel (1g) when the drop’s viscosity is taken to be infinite in the rigid-particle limit. The memory kernels of this sort can also occur to nearly spherical rigid particles having small asphericity in particle shape<sup>40,41</sup> or to stick–slip Janus spheres.<sup>30</sup> However, in the special case where a viscous drop becomes an inviscid bubble, the singular Basset kernel completely vanishes, making the entire memory kernel governed solely by the regular non-Basset kernel.<sup>31,32</sup>

Now, turn the attention to a partial slip particle. Its memory force kernel takes the same functional form (2) as that for a full slip bubble.<sup>22</sup> Given that the difference between a partial slip particle and a full slip bubble is merely the extent of slip and also that both have the same Mittag–Leffler type of memory kernels, one might think that not much difference in the physics exists between the two. Actually, this is not true. The reason is that the values of  $\gamma$  in (2) for these two cases, which control the respective temporal attenuation rates of their memory kernels, turn out to be rather different in terms of the associated time and length scales. In the bubble case,  $\gamma_{bubble} \sim \nu/a^2$ , corresponding to the typical viscous relaxation time across the particle size  $a$ . For the slip case, on the contrary, especially when the slip length  $\lambda$  is much smaller than  $a$ ,  $\gamma_{slip} \sim \nu/\lambda^2$  is not characterized by  $a$  but by  $\lambda$ ,<sup>22,29</sup> corresponding to the slip–stick transition time. This disparity in the time scales implies that the detailed particle dynamics of these two cases likely differ qualitatively. This observation also implies that even though memory kernels take the same functional form, they do not necessarily imply the same physics.

It actually turns out in the study by Premlata and Wei<sup>22</sup> that the non-Basset force kernel due to slip involves two distinct time scales: the slip–stick transition time  $t_\lambda = \lambda^2/\nu$  and the viscous relaxation time  $t_\nu = a^2/\nu$ , controlling short-time and long-time force behaviors for a slip particle, respectively. In fact,  $t_\lambda$  marks the moment when the boundary layer changes from being thin to being thick with respect to the slip length  $\lambda$ . Its impacts on the history force have been illustrated with a slip sphere moving suddenly from rest to a constant

velocity, showing that the force on the sphere can exhibit a constant plateau for time  $t$  shorter than  $t_\lambda$  followed by a  $t^{1/2}$  decay prior to the Basset  $t^{-1/2}$  attenuation during a much longer relaxation period of  $t_v$ . This is very different from the Basset force that always decays as  $t^{-1/2}$  for a no-slip sphere.

As such, if a slip particle does not undergo an impulsive motion but is propelled by an external force or advected by a time-dependent imposed flow, we anticipate that its unsteady motion will behave rather differently than that of a no-slip particle or fluid particle. In this work, we thus look at possible characteristic changes in unsteady particle motion in terms of changes in history force/torque from the Basset type to non-Basset type due to slip effects. To this end, we notice that the unsteady Faxen formulas with slip have been reported previously for the force and torque on a slip particle.<sup>23–26</sup> However, these formulas are somewhat incomplete since they involve the unresolved surface and volume integrals of the background flow velocity and moment over a particle without making finite-size effects explicit in the standard Faxen form. Hence, it is less convenient to apply them directly to demonstrate the non-Basset particle dynamics by solving the Maxey–Riley-type equations of motion in the presence of background flows. In order to provide a more systematic account for how a slip particle responds to an external forcing or to an imposed flow, instead of using these previously established Faxen formulas directly, we will rederive them not only to obtain the non-Basset kernels needed for determining the particle motion but also to capture finite-size effects that resulted from an imposed flow. The equations of the particle motion will also be derived in line by modifying the classical Maxey–Riley equation.

Along the lines above, the paper is organized as follows: In Secs. II–IV, we first establish Faxen’s formulas and the modified Maxey–Riley type equations, providing the framework needed for determining the motion of a slip particle in an arbitrary time-dependent Stokes flow. In Sec. V, we find that while the changes in these formulas and equations may appear in mathematical formality, the impacts are actually substantial in physics. We inspect unsteady motion responses of a slip particle for a number of situations, showing that a fraction of slip can make the particle motion responses qualitatively different from those of a no-slip particle and to a full slip bubble. For transient motion, the differences are found to mainly manifest in the short time regime due to the atypical non-Basset kernels brought by slip, showing that the translational and angular velocities of a slip particle can vary with time in different powers compared to those of single no-slip particles. Dynamic distinctions of a slip particle to a full slip bubble become even more evident in an oscillatory vortical flow, showing that an additional inertial torque can be introduced by slip effects through the new Faxen term. In Sec. VI, we conclude this work and discuss potential impacts of our findings in broader perspectives.

## II. HYDRODYNAMIC FORCE AND TORQUE ON A SLIP SPHERE IN AN UNSTEADY STOKES FLOW

Although the unsteady Faxen formulas for a slip sphere have been reported previously by several authors, we still feel the need to rederive them after reviewing these early developments below. Albano *et al.*<sup>25</sup> and Felderhof<sup>26</sup> derived their results

in terms of Fourier frequency using the induced force density approach by redistributing a point force over the surface of a sphere. Pienkowska<sup>24</sup> used the same approach to rederive the formulas in terms of time, showing non-Basset history terms due to slip effects. Gatignol<sup>23</sup> used the reciprocal theorem to arrive at essentially the same results as those mentioned above. However, in all these early developments, the results were expressed in terms of surface and volume average quantities over a sphere. In other words, their results did not make finite-size effects explicit in terms of additional Faxen terms by expanding the quantities at the sphere’s center. This makes their formulas less convenient to evaluate the force and torque on a sphere in the presence of background flows. In this work, we remedy this issue by re-formulating the derivations. In the first step, we apply the reciprocal theorem<sup>42</sup> to develop general formulas below for the force and torque exerted on a slip sphere.

Consider the unsteady fluid motion around a slip spherical particle of radius  $a$  in an incompressible Newtonian fluid of density  $\rho$  and viscosity  $\mu$ . Let  $(\hat{\mathbf{u}}, \hat{\boldsymbol{\sigma}})e^{-i\omega t}$  be the fluid velocity and stress fields, where  $\omega$  is the oscillation frequency and  $t$  is the time. At a small particle Reynolds number, the equations of motion in Fourier space are

$$\nabla \cdot \hat{\mathbf{u}} = 0, \tag{3}$$

$$\nabla \cdot \hat{\boldsymbol{\sigma}} = -i\omega\rho\hat{\mathbf{u}}, \tag{4}$$

where the stress is  $\hat{\boldsymbol{\sigma}} = -\mathbf{I}\hat{p} + \mu(\nabla\hat{\mathbf{u}} + \nabla\hat{\mathbf{u}}^T)$ , with  $\hat{p}$  being the dynamic pressure. Let  $(\hat{\mathbf{u}}_1, \hat{\boldsymbol{\sigma}}_1)$  and  $(\hat{\mathbf{u}}_2, \hat{\boldsymbol{\sigma}}_2)$  be two flow solutions satisfying (3) and (4) subject to the same type of boundary conditions. Working with reciprocal operations  $\hat{\mathbf{u}}_1 \cdot (\nabla \cdot \hat{\boldsymbol{\sigma}}_2) = \nabla \cdot (\hat{\mathbf{u}}_1 \cdot \hat{\boldsymbol{\sigma}}_2) - \nabla\hat{\mathbf{u}}_1 : \hat{\boldsymbol{\sigma}}_2$  and  $\hat{\mathbf{u}}_2 \cdot (\nabla \cdot \hat{\boldsymbol{\sigma}}_1) = \nabla \cdot (\hat{\mathbf{u}}_2 \cdot \hat{\boldsymbol{\sigma}}_1) - \nabla\hat{\mathbf{u}}_2 : \hat{\boldsymbol{\sigma}}_1$ , the subtraction between them yields

$$\nabla \cdot (\hat{\mathbf{u}}_1 \cdot \hat{\boldsymbol{\sigma}}_2) - \hat{\mathbf{u}}_1 \cdot (\nabla \cdot \hat{\boldsymbol{\sigma}}_2) = \nabla \cdot (\hat{\mathbf{u}}_2 \cdot \hat{\boldsymbol{\sigma}}_1) - \hat{\mathbf{u}}_2 \cdot (\nabla \cdot \hat{\boldsymbol{\sigma}}_1). \tag{5}$$

Integrating (5) over the volume enclosing the particle and applying the divergence theorem with the assumption that the velocity and stress vanish at infinity, (5) becomes

$$\begin{aligned} \int_{S_p} \hat{\mathbf{u}}_1 \cdot (\hat{\boldsymbol{\sigma}}_2 \cdot \mathbf{n})dS + \int_{\mathcal{V}} \hat{\mathbf{u}}_1 \cdot (\nabla \cdot \hat{\boldsymbol{\sigma}}_2)d\mathcal{V} \\ = \int_{S_p} \hat{\mathbf{u}}_2 \cdot (\hat{\boldsymbol{\sigma}}_1 \cdot \mathbf{n})dS + \int_{\mathcal{V}} \hat{\mathbf{u}}_2 \cdot (\nabla \cdot \hat{\boldsymbol{\sigma}}_1)d\mathcal{V}, \end{aligned} \tag{6}$$

where  $S_p$  is the particle surface with  $\mathbf{n}$  being the unit normal vector pointing outward and  $\mathcal{V}$  is the volume outside the particle. For the volume integral terms in (6), replacing  $\nabla \cdot \hat{\boldsymbol{\sigma}}$  by  $-i\omega\rho\hat{\mathbf{u}}$  using (4), we find that they are identical and thus canceled out. For arbitrary time-dependent flows, the problems can be formulated using Laplace transform in terms of the Laplace variable  $s = -i\omega$ . In this case, these two volume integrals can only be eliminated under the condition that the flows start from rest with  $\mathbf{u}_1(t = 0^-) = 0$  and  $\mathbf{u}_2(t = 0^-) = 0$ .<sup>8</sup> In other words, the two volume integrals can be eliminated in either steady oscillatory flows or flows starting from rest. In any case, (6) is reduced to the well-known reciprocal relationship,

$$\int_{S_p} \hat{\mathbf{u}}_1 \cdot (\hat{\boldsymbol{\sigma}}_2 \cdot \mathbf{n})dS = \int_{S_p} \hat{\mathbf{u}}_2 \cdot (\hat{\boldsymbol{\sigma}}_1 \cdot \mathbf{n})dS. \tag{7}$$

Equation (7) allows us to determine the force and the torque for the desired problem (denoted as Problem 2) using the solution to the auxiliary problem (denoted as Problem 1). For the latter, we choose the particle undergoing translation with velocity  $Ue^{-i\omega t}$  or/and rotation with angular velocity  $\Omega e^{-i\omega t}$  in a quiescent fluid [see Fig. 1(a)]. In the former, we seek the force/torque on the particle that translates/rotates at the same velocity/angular velocity in a non-uniform imposed flow  $\mathbf{u}^\infty e^{-i\omega t}$  with the corresponding stress field  $\boldsymbol{\sigma}^\infty e^{-i\omega t}$  [see Fig. 1(b)]. For this problem, the disturbed flow field can be written as  $(\hat{\mathbf{u}}_2, \hat{\boldsymbol{\sigma}}_2) = (\mathbf{u}_2, \boldsymbol{\sigma}_2) - (\mathbf{u}^\infty, \boldsymbol{\sigma}^\infty)$  with respect to the imposed flow. For either problem, aside from the vanishing fluid velocity at infinity, each is subject to the impenetration and the Navier-slip (with the slip length  $\lambda$ ) boundary conditions on the particle surface  $|\mathbf{x}| = a$  as follows:<sup>22,43</sup>

For Problem 1,

$$(\hat{\mathbf{u}}_1 - \mathbf{U} - \boldsymbol{\Omega} \times \mathbf{x}) \cdot (\mathbf{I} - \mathbf{nn}) = \frac{\lambda}{\mu} (\hat{\boldsymbol{\sigma}}_1 \cdot \mathbf{n}) \cdot (\mathbf{I} - \mathbf{nn}), \quad (8)$$

$$(\hat{\mathbf{u}}_1 - \mathbf{U} - \boldsymbol{\Omega} \times \mathbf{x}) \cdot \mathbf{n} = 0. \quad (9)$$

For Problem 2,

$$\begin{aligned} & (\hat{\mathbf{u}}_2 - \mathbf{U} - \boldsymbol{\Omega} \times \mathbf{x} + \mathbf{u}^\infty) \cdot (\mathbf{I} - \mathbf{nn}) \\ &= \frac{\lambda}{\mu} [(\hat{\boldsymbol{\sigma}}_2 \cdot \mathbf{n}) + (\boldsymbol{\sigma}^\infty \cdot \mathbf{n})] \cdot (\mathbf{I} - \mathbf{nn}), \end{aligned} \quad (10)$$

$$(\hat{\mathbf{u}}_2 - \mathbf{U} - \boldsymbol{\Omega} \times \mathbf{x} + \mathbf{u}^\infty) \cdot \mathbf{n} = 0. \quad (11)$$

To provide the formulas for evaluating the force and the torque on the particle, we first rewrite the left-hand side of (7) as

$$\begin{aligned} & \int_{S_p} (\mathbf{U} + \boldsymbol{\Omega} \times \mathbf{x}) \cdot (\hat{\boldsymbol{\sigma}}_2 \cdot \mathbf{n}) dS \\ &+ \int_{S_p} (\hat{\mathbf{u}}_1 - \mathbf{U} - \boldsymbol{\Omega} \times \mathbf{x}) \cdot (\hat{\boldsymbol{\sigma}}_2 \cdot \mathbf{n}) dS. \end{aligned} \quad (12)$$

In the second integral of the above, because of (8) and (9),  $(\hat{\mathbf{u}}_1 - \mathbf{U} - \boldsymbol{\Omega} \times \mathbf{x}) \cdot (\mathbf{I} - \mathbf{nn})$  can be replaced by  $(\lambda/\mu)(\hat{\boldsymbol{\sigma}}_1 \cdot \mathbf{n}) \cdot (\mathbf{I} - \mathbf{nn})$ . Hence, (12) can be re-expressed as

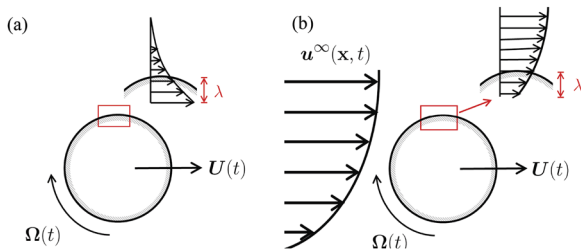


**FIG. 1.** The selected problems for applying the reciprocal theorem. (a) The auxiliary problem: a slip particle translating/rotating unsteadily in a quiescent fluid. (b) The problem of interest: a slip particle moving unsteadily at the same translational velocity/angular velocity in a time-dependent non-uniform imposed flow.

$$\begin{aligned} & \mathbf{U} \cdot \int_{S_p} (\hat{\boldsymbol{\sigma}}_2 \cdot \mathbf{n}) dS + \boldsymbol{\Omega} \cdot \int_{S_p} (\mathbf{x} \times (\hat{\boldsymbol{\sigma}}_2 \cdot \mathbf{n})) dS \\ &+ \frac{\lambda}{\mu} \int_{S_p} (\hat{\boldsymbol{\sigma}}_1 \cdot \mathbf{n}) \cdot (\mathbf{I} - \mathbf{nn}) \cdot (\boldsymbol{\sigma}_2 \cdot \mathbf{n}) dS. \end{aligned} \quad (13)$$

Next, we consider the right-hand side of (7). It can be recasted as

$$\begin{aligned} & \int_{S_p} (\hat{\mathbf{u}}_2 - \mathbf{U} - \boldsymbol{\Omega} \times \mathbf{x} + \mathbf{u}^\infty) \cdot (\hat{\boldsymbol{\sigma}}_1 \cdot \mathbf{n}) dS \\ &+ \int_{S_p} (\mathbf{U} + \boldsymbol{\Omega} \times \mathbf{x} - \mathbf{u}^\infty) \cdot (\hat{\boldsymbol{\sigma}}_1 \cdot \mathbf{n}) dS. \end{aligned} \quad (14)$$

In the first integral of the above, we make use of (10) and (11) to rewrite  $(\hat{\mathbf{u}}_2 - \mathbf{U} - \boldsymbol{\Omega} \times \mathbf{x} + \mathbf{u}^\infty) \cdot (\mathbf{I} - \mathbf{nn})$  as  $(\lambda/\mu)((\hat{\boldsymbol{\sigma}}_2 \cdot \mathbf{n}) + (\boldsymbol{\sigma}^\infty \cdot \mathbf{n})) \cdot (\mathbf{I} - \mathbf{nn})$ , turning (14) into

$$\begin{aligned} & \frac{\lambda}{\mu} \int_{S_p} (\hat{\boldsymbol{\sigma}}_1 \cdot \mathbf{n}) \cdot (\mathbf{I} - \mathbf{nn}) \cdot (\hat{\boldsymbol{\sigma}}_2 \cdot \mathbf{n}) dS \\ &+ \frac{\lambda}{\mu} \int_{S_p} (\boldsymbol{\sigma}^\infty \cdot \mathbf{n}) \cdot (\mathbf{I} - \mathbf{nn}) \cdot (\hat{\boldsymbol{\sigma}}_1 \cdot \mathbf{n}) dS \\ &+ \int_{S_p} (\mathbf{U} + \boldsymbol{\Omega} \times \mathbf{x} - \mathbf{u}^\infty) \cdot (\hat{\boldsymbol{\sigma}}_1 \cdot \mathbf{n}) dS. \end{aligned} \quad (15)$$

Combining (13) and (15), the two identical integrals  $(\lambda/\mu)(\hat{\boldsymbol{\sigma}}_1 \cdot \mathbf{n}) \cdot (\mathbf{I} - \mathbf{nn}) \cdot (\hat{\boldsymbol{\sigma}}_2 \cdot \mathbf{n})$  are canceled out. This allows us to write the force  $\mathcal{F} = \int_{S_p} (\hat{\boldsymbol{\sigma}}_2 \cdot \mathbf{n}) dS$  and the torque  $\mathcal{T} = \int_{S_p} \mathbf{x} \times (\hat{\boldsymbol{\sigma}}_2 \cdot \mathbf{n}) dS$  in terms of the surface traction  $(\hat{\boldsymbol{\sigma}}_1 \cdot \mathbf{n})$  and the ambient flow quantities,

$$\begin{aligned} & \mathbf{U} \cdot \mathcal{F} + \boldsymbol{\Omega} \cdot \mathcal{T} = \int_{S_p} (\mathbf{U} + \boldsymbol{\Omega} \times \mathbf{x} - \mathbf{u}^\infty) \cdot (\hat{\boldsymbol{\sigma}}_1 \cdot \mathbf{n}) dS \\ &+ \frac{\lambda}{\mu} \int_{S_p} (\hat{\boldsymbol{\sigma}}_1 \cdot \mathbf{n}) \cdot (\mathbf{I} - \mathbf{nn}) \cdot (\boldsymbol{\sigma}^\infty \cdot \mathbf{n}) dS. \end{aligned} \quad (16)$$

We notice that Eq. (16) derived by far is not limited to a sphere but applicable to a particle of an arbitrary shape. Let  $(\mathbf{U} + \boldsymbol{\Omega} \times \mathbf{x} - \mathbf{u}^\infty) \equiv \hat{\mathbf{u}}^\infty$  and further write  $(\hat{\boldsymbol{\sigma}}_1 \cdot \mathbf{n})$  in terms of the translation resistance density matrix  $\mathcal{R}^T$  and the rotation resistance density matrix  $\mathcal{R}^R$ ,

$$(\hat{\boldsymbol{\sigma}}_1 \cdot \mathbf{n}) = (\hat{\boldsymbol{\sigma}}^T \cdot \mathbf{n}) + (\hat{\boldsymbol{\sigma}}^R \cdot \mathbf{n}) = \mathcal{R}^T \cdot \mathbf{U} + \mathcal{R}^R \cdot (\boldsymbol{\Omega} \times \mathbf{x}). \quad (17)$$

For an isotropic sphere in an unbounded flow, there will be no translation-rotation coupling, allowing us to determine  $\mathcal{F}$  and  $\mathcal{T}$  as

$$\mathcal{F} = \int_{S_p} \mathcal{R}^T \cdot \left[ \hat{\mathbf{u}}^\infty + \frac{\lambda}{\mu} (\mathbf{I} - \mathbf{nn}) \cdot (\boldsymbol{\sigma}^\infty \cdot \mathbf{n}) \right] dS, \quad (18)$$

$$\mathcal{T} = \int_{S_p} \mathbf{x} \times \left[ \mathcal{R}^R \cdot \left( \hat{\mathbf{u}}^\infty + \frac{\lambda}{\mu} (\mathbf{I} - \mathbf{nn}) \cdot (\boldsymbol{\sigma}^\infty \cdot \mathbf{n}) \right) \right] dS. \quad (19)$$

Equations (18) and (19) are essentially the starting formulas derived by Gatignol<sup>23</sup> [see his Eq. (22)], consisting of two contributions: the slip velocity  $\hat{\mathbf{u}}^\infty$  and the slip stress  $(\mathbf{I} - \mathbf{nn}) \cdot (\boldsymbol{\sigma}^\infty \cdot \mathbf{n})$  exerted by the background flow. It is clear that for  $\lambda = 0$ , the slip stress part

vanishes, making (18) and (19) reduced to the usual formulas for no-slip sphere. Recall that the previous Faxen formulas are written in terms of the surface integrals of the background flow velocity and moment over a sphere.<sup>23,24</sup> These integrals come from  $\mathbf{u}^\infty$  and  $\boldsymbol{\sigma}^\infty$ , as clearly seen in (18) and (19). In Secs. III and IV, we will re-express these integrals in the Faxen form by expanding  $\mathbf{u}^\infty$  and  $\boldsymbol{\sigma}^\infty$  at the sphere's center. It actually turns out that such calculations are highly non-trivial, as they can involve even moment surface integrals up to  $\mathbf{nnnnnn}$ , especially in the derivation of the Faxen second law for the torque (see Sec. IV).

We remark that the steady force and torque formulas obtained by Keh and Chen<sup>43</sup> are also identical to (18) and (19). In their formulas, the slip stress part  $(\lambda/\mu)(\hat{\boldsymbol{\sigma}}_1 \cdot \mathbf{n}) \cdot (\mathbf{I} - \mathbf{nn}) \cdot (\boldsymbol{\sigma}^\infty \cdot \mathbf{n})$  in (16) is replaced by  $(\hat{\mathbf{u}}_1 - \mathbf{U} - \boldsymbol{\Omega} \times \mathbf{x}) \cdot (\boldsymbol{\sigma}^\infty \cdot \mathbf{n})$ , since the traction  $(\hat{\boldsymbol{\sigma}}_1 \cdot \mathbf{n})$  in the unsteady case, because of  $-i\omega\rho\hat{\mathbf{u}}$  in (4), takes a very different form than that in the steady case. This is why additional history and added mass terms will arise in the unsteady force and torque.

Aside from Faxen's first and second laws for particle force and torque, there is also Faxen's third law for the particle stresslet. Such a law can be used to calculate the effective viscosity of a particle suspension since it was first derived by Batchelor and Green.<sup>44</sup> Extensions have been made for slip spheres,<sup>43</sup> composite spheres,<sup>45</sup> and stick-slip Janus spheres<sup>46,47</sup> under the steady situation. For the unsteady situation, a modified Faxen third law for slip spheres can, in principle, be derived using a formula similar to that of Keh and Chen<sup>43</sup> but with  $(\hat{\mathbf{u}}_1, \hat{\boldsymbol{\sigma}}_1)$  in a linear flow field in terms of the unsteady stresslet.<sup>48</sup> This law can be used to study the rheology of a suspension of inertial self-propelled sphere swimmers on which the hydrodynamic force and torque do not vanish because of unsteadiness.<sup>2</sup> This is a topic worth investigating but beyond the scope of the present work, which will be pursued in our future study.

### III. MODIFIED FAXEN FORCE LAW AND MAXEY-RILEY EQUATION FOR A SLIP SPHERE

To evaluate the force from (18), it first requires the translation resistance density matrix by solving Problem 1 (see Appendix A for detailed derivation),

$$\mathcal{R}^T = -\frac{3\mu}{2a} \left[ \frac{\alpha + 1}{\hat{\lambda}(\alpha + 3) + 1} \right] \mathbf{I} - \frac{\mu}{2a} \left[ \frac{18(\alpha + 1)\hat{\lambda}}{\hat{\lambda}(\alpha + 3) + 1} + \alpha^2 \right] \mathbf{nn}, \quad (20)$$

where  $\alpha^2 = -i\omega a^2/\nu$  is the dimensionless complex frequency, with  $\nu = \mu/\rho$  being the kinematic viscosity, and  $\hat{\lambda} = \lambda/a$  is the dimensionless slip length. Next, we expand  $\mathbf{u}^\infty$  and  $\boldsymbol{\sigma}^\infty$  at the sphere's center,

$$\mathbf{u}^\infty = \mathbf{u}^\infty(0) + \mathbf{x} \cdot \nabla \mathbf{u}^\infty|_0 + \frac{\mathbf{x} \cdot \mathbf{x}}{2} : \nabla \nabla \mathbf{u}^\infty|_0 + \dots, \quad (21)$$

$$\boldsymbol{\sigma}^\infty = \boldsymbol{\sigma}^\infty(0) + \mathbf{x} \cdot \nabla \boldsymbol{\sigma}^\infty|_0 + \frac{\mathbf{x} \cdot \mathbf{x}}{2} : \nabla \nabla \boldsymbol{\sigma}^\infty|_0 + \dots. \quad (22)$$

Because  $\boldsymbol{\Omega} \times \mathbf{x}$  makes no contribution to the force, we can substitute (20)–(22) with  $\mathbf{u}^\infty = \mathbf{U} - \mathbf{u}^\infty$  into (18). The  $\mathbf{u}^\infty$  term in (18) gives

$$\begin{aligned} & 4\pi a^2 \left( \frac{-3\mu}{2a} \right) \left[ \frac{\alpha + 1}{\hat{\lambda}(\alpha + 3) + 1} \right] \mathbf{u}^\infty(0) \\ & + \frac{4}{3} \pi a^2 \left( \frac{-\mu}{2a} \right) \left[ \frac{18(\alpha + 1)\hat{\lambda}}{\hat{\lambda}(\alpha + 3) + 1} + \alpha^2 \right] \mathbf{u}^\infty(0) \\ & + \frac{4}{3} \pi a^4 \left( \frac{-3\mu}{4a} \right) \left[ \frac{\alpha + 1}{\hat{\lambda}(\alpha + 3) + 1} \right] \nabla^2 \mathbf{u}^\infty|_0 \\ & + \frac{4}{15} \pi a^4 \left( \frac{-\mu}{4a} \right) \left[ \frac{18(\alpha + 1)\hat{\lambda}}{\hat{\lambda}(\alpha + 3) + 1} + \alpha^2 \right] \nabla^2 \mathbf{u}^\infty|_0. \end{aligned} \quad (23)$$

The slip term in (18) contributes to a force of

$$\begin{aligned} & \left( \frac{-3\mu}{2a} \right) \left[ \frac{\alpha + 1}{\hat{\lambda}(\alpha + 1) + 1} \right] \left( \frac{\lambda}{\mu} \right) \left[ \frac{4}{3} \pi a^3 \nabla \cdot \boldsymbol{\sigma}^\infty|_0 \right. \\ & \left. - \frac{4}{15} \pi a^3 (2\nabla \cdot \boldsymbol{\sigma}^\infty|_0 + \nabla \boldsymbol{\sigma}_{ii}^\infty|_0) \right]. \end{aligned} \quad (24)$$

In deriving (23) and (24), we have used the identities  $\int_{S_p} n_i n_j dS = (4\pi a^2/3)\delta_{ij}$  and  $\int_{S_p} n_i n_j n_k n_m dS = (4\pi a^2/15)[\delta_{ij}\delta_{km} + \delta_{ik}\delta_{jm} + \delta_{im}\delta_{jk}]$ . Combining (23) and (24) together with  $\nabla \boldsymbol{\sigma}_{ii}^\infty = -3\nabla p^\infty$ ,  $\nabla \cdot \boldsymbol{\sigma}^\infty + \nabla p^\infty = \mu \nabla^2 \mathbf{u}^\infty$ , and  $\nabla^2 \mathbf{u}^\infty = -\nabla^2 \hat{\mathbf{u}}^\infty$ , we obtain the Faxen first law for the force,

$$\begin{aligned} \frac{\mathcal{F}}{-6\pi\mu a} &= \left( \Lambda + \frac{\Lambda^2 \alpha}{1 + \beta\alpha} \right) \left[ 1 + \frac{a^2}{6(1 + 2\hat{\lambda})} \nabla^2 \right] \mathbf{u}^\infty|_0 \\ &+ \frac{\alpha^2}{9} \left[ 1 + \frac{a^2}{10} \nabla^2 \right] \mathbf{u}^\infty|_0, \end{aligned} \quad (25)$$

where  $\Lambda = (1 + 2\hat{\lambda})/(1 + 3\hat{\lambda})$  is the analogous Hadamard–Rybczynski factor for the Stokes drag and  $\beta = \hat{\lambda}/(1 + 3\hat{\lambda})$ , as will become clear later, can be thought of as the slip coefficient for the history force. Equation (25) agrees with the previous force formula that involves the surface and volume averages of the fluid velocity within the sphere.<sup>25,26</sup> Here, we turn these averages explicitly into the Faxen form.

To convert (25) in terms of time  $t/t_v$  with respect to the viscous relaxation time  $t_v = a^2/\nu$ , we let  $\alpha^2 = -i\omega t_v = s$  to rewrite (25) in terms of the Laplace variable  $s$ ,

$$\begin{aligned} \frac{\mathcal{F}(s)}{-6\pi\mu a} &= \left[ \frac{\Lambda}{s} + \Lambda^2 G(s) \right] s \left[ 1 + \frac{a^2}{6(1 + 2\hat{\lambda})} \nabla^2 \right] \mathbf{u}^\infty|_0 \\ &+ \frac{s}{9} \left[ 1 + \frac{a^2}{10} \nabla^2 \right] \mathbf{u}^\infty|_0, \end{aligned} \quad (26)$$

where  $G(s) = 1/(s^{1/2} + \beta s)$ . Performing an inverse Laplace transform and making use of the convolution theorem  $\mathcal{L}^{-1}\{G(s)s f(s)\} = \int_0^t G(t-t') df(t')/dt' dt' + G(t)f(t=0)$  with the memory kernel

$$\begin{aligned} G(t) &= \mathcal{L}^{-1} \left[ \frac{1}{s^{1/2}(1 + \beta s^{1/2})} \right] \\ &= \beta^{-1} \exp(\beta^{-2} t/t_v) \operatorname{erfc}(\beta^{-1} \sqrt{t/t_v}), \end{aligned} \quad (27)$$

we convert (26) into

$$\begin{aligned} \frac{\mathcal{F}(t)}{-6\pi\mu a} = & \Lambda \left[ 1 + \frac{a^2}{6(1+2\hat{\lambda})} \nabla^2 \right] \hat{\mathbf{u}}^\infty(t)|_0 + \frac{1}{9} \frac{d}{dt} \left[ 1 + \frac{a^2}{10} \nabla^2 \right] \hat{\mathbf{u}}^\infty(t)|_0 \\ & + \Lambda^2 \left\{ \int_0^t G(t-t') \frac{d}{dt'} \left[ 1 + \frac{a^2}{6(1+2\hat{\lambda})} \nabla^2 \right] \hat{\mathbf{u}}^\infty(t')|_0 dt' \right. \\ & \left. + G(t) \left[ 1 + \frac{a^2}{6(1+2\hat{\lambda})} \nabla^2 \right] \hat{\mathbf{u}}^\infty(t=0^-)|_0 \right\}. \end{aligned} \quad (28)$$

Equation (28) essentially recovers the previous force formula<sup>23,24</sup> with the surface and volume averages of the fluid velocity now being expanded into the Faxen terms. In (28), the first term is the instantaneous Stokes drag, in agreement with that obtained by Ref. 43. The second term recovers the added mass in the equation derived by Ref. 8. This term is purely of the potential-flow origin regardless of whether a particle is slip or not. The third term represents the non-Basset history force. It consists of two parts. The first part is the memory integral involving the kernel (27) with the additional Faxen correction when slip is present. This part without the Faxen correction also recovers the memory integral obtained previously.<sup>22–24</sup> The second part accounts for the mismatch between the initial particle velocity and the initial flow velocity,  $\mathbf{U}(t=0^-) - (1 + [6(1+2\hat{\lambda})]^{-1} a^2 \nabla^2) \mathbf{u}^\infty(t=0^-)|_0$ . In the no-slip limit in which  $\hat{\lambda} = 0$  and  $G$  becomes the Basset kernel  $(1/\sqrt{\pi})(t_v/t)^{1/2}$ , (28) is reduced to the result obtained previously.<sup>8,9</sup>

Figure 2 plots how the slip-induced non-Basset kernel  $G$  varies with time  $t$ . This is equivalent to looking at the temporal response of the history force on a slip sphere when it moves suddenly from rest to a constant velocity.<sup>22</sup> As shown in Fig. 2,  $G$  can display a number of different features compared to the no-slip Basset kernel  $G_B = (1/\sqrt{\pi})(t_v/t)^{1/2}$ . First of all,  $G$  is finite at  $t = 0$  as opposed to  $G_B$ . This makes the former decay with time less rapidly than the

latter, as shown in Fig. 2(a). Looking into its short-time asymptotic behavior,

$$G(t) = \beta^{-1} \left[ 1 - \frac{2}{\sqrt{\pi}} \left( \frac{t}{\beta^2 t_v} \right)^{1/2} \right] + O(t/t_v), \quad (29)$$

such a non-singular characteristic of  $G$  actually comes from the constant  $\beta^{-1} = \hat{\lambda}^{-1} + 3$  as  $t \rightarrow 0$ . The constant is attributed to the constant shear stress that resulted from strong slip effects when the viscous boundary layer  $\delta \sim (vt)^{1/2}$  is much thinner than the slip length  $\lambda$ .<sup>22,49</sup> When  $\hat{\lambda}$  is small, in particular, (29) reduces to

$$G(t) \approx \hat{\lambda}^{-1} \left[ 1 - \frac{2}{\sqrt{\pi}} \left( \frac{t}{t_\lambda} \right)^{1/2} \right] + O(t/t_\lambda). \quad (30)$$

Rather than by the viscous relaxation time  $t_v = a^2/\nu$ ,  $G$  is now characterized by the slip–stick transition time  $t_\lambda = \hat{\lambda}^2 t_v = \lambda^2/\nu$  corresponding to the time scale when  $\delta \sim (vt)^{1/2}$  grows to the size of  $\lambda$ . Compared to the no-slip Basset kernel  $G_B$  that is singular at  $t = 0$ , (30) reveals that even if the amount of slip is small, the memory kernel is regular at  $t = 0$ . This means that adding slip changes the memory kernel from singular type to regular type. As also indicated by (30) and shown in Fig. 2(b),  $G$  will start with a constant value. The constant continues until  $t_\lambda$  after which  $G$  declines with time. At times longer than  $t_v$ ,  $G = (1/\sqrt{\pi})(t_v/t)^{1/2} + O((t_v/t)^{3/2})$  and recovers  $G_B$  as  $t \rightarrow \infty$ . In other words,  $G$  involves two time scales:  $t_\lambda = \lambda^2/\nu$  and  $t_v = a^2/\nu$ , controlling the short-term and the long-term responses of a slip particle, respectively. These features of  $G$  are very distinct from  $G_B$ , which is characterized solely by  $t_v$  and always falls off as  $(t_v/t)^{1/2}$ . It is worth mentioning that an additional non-Basset memory kernel like (27) can also be introduced by either asphericity<sup>40,41</sup> or fluidity.<sup>31,32</sup> However, unlike the single memory kernel (27) brought by slip, the total memory kernel in either situation still includes singular  $G_B$  and hence becomes diverging as  $t \rightarrow 0$ . An exception is the bubble case

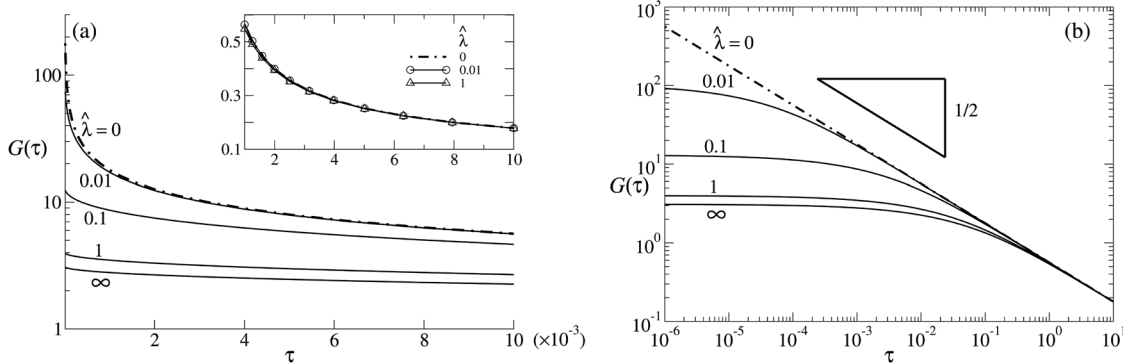


**FIG. 2.** Temporal response of the non-Basset memory kernel  $G$  given by (27) for the unsteady translation of a single slip sphere. (a) Plot of  $G$  against time  $\tau = t/t_v$ , normalized by the viscous time  $t_v$ , for different values of the slip length  $\hat{\lambda}$ . At  $\hat{\lambda} = 0$ ,  $G$  is reduced to the Basset kernel  $G_B = 1/(\pi\tau)^{1/2}$  (dashed-dotted line). Increasing  $\hat{\lambda}$  lowers  $G$ . However, at sufficiently long times,  $G$  recovers  $G_B$  regardless of  $\hat{\lambda}$ , as shown in the inset. (b) Log–log plot of  $G$  vs  $\tau$ . At a sufficiently short time,  $G$  at a given  $\hat{\lambda}$  keeps a constant level, in contrast to  $G_B$  that diverges as  $\tau \rightarrow 0$ . When  $\tau$  is increased to a certain point,  $G$  will start to turn toward  $G_B$ , signifying a slip–stick transition (SST) at around the crossover time  $\tau \sim \hat{\lambda}^2$  between the short-time plateau and the  $\tau^{-1/2}$  Basset decay. Increasing  $\hat{\lambda}$  not only lowers the level of  $G$  in the short-time regime but also delays the SST time. Although  $G$  for a full slip bubble with  $\hat{\lambda} \rightarrow \infty$  also takes the same functional form like (27), it does not have SST like that for a partial slip particle.

whose memory kernel is  $G_{bubble} = 3 \exp(9(t/t_v)) \operatorname{erfc}(3(t/t_v)^{1/2})$ ,<sup>31</sup> as can also be obtained from (27) by taking the  $\hat{\lambda} \rightarrow \infty$  limit. In this case,  $G_{bubble}$  remains finite at  $t = 0$ . However, for  $t > 0$ ,  $G_{bubble}$  will decrease monotonically with time in the usual time scale  $t_v$ . Hence, it will not display any slip–stick transition like the slip case described by (27). This is the main difference between a partial slip particle and a full slip bubble.

Another remark worth making is that while there is a hydrodynamic analogy in the Stokes drag between a slip particle and a viscous drop,<sup>22,50</sup> there is no such analogy for the history force. The reason is that the memory kernel for the drop case generally does not reduce to that for the slip case. Specifically, because of fluid slippage on the surface of a slip particle, the particle's momentum can be dissipated by the finite viscous stress brought by slip upon the start of the particle's motion.<sup>49</sup> For a viscous drop, however, its momentum can only be dissipated within the thin viscous boundary layers developing inside and outside the drop in the vicinity of the drop surface, and the stresses associated with these layers are enormous in the beginning of the drop's motion. It is also this reason why the memory kernel for the slip case is purely of the non-Basset type and remains finite at  $t = 0$ , whereas that for the drop case further includes a Basset kernel and is thus singular at  $t = 0$ .<sup>32</sup>

In view of the above, such a non-Basset  $G$  brought by slip is distinct from those by asphericity and fluidity. As will be demonstrated in Sec. V, this new memory kernel will result in completely different motion responses for a slip particle, especially in the short-time regime in which the resultant history force often dominates when the slip length  $\lambda$  is small.

Following Ref. 8, we can add the hydrodynamic force (28) to the force balance over a slip sphere, modifying the Maxey–Riley equation of motion (1) to

$$m_p \frac{d\mathbf{U}}{dt} = F_{ex} + m_f \left. \frac{D\mathbf{u}^\infty}{Dt} \right|_{X(t)} - \frac{m_f}{2} \frac{d}{dt} \left[ \mathbf{U} - \mathbf{u}^\infty(\mathbf{X}(t), t) - \frac{a^2}{10} \nabla^2 \mathbf{u}^\infty \right]_{X(t)} - 6\pi\mu a \Lambda \mathbf{W} - 6\pi\mu a \Lambda^2 \left[ \int_0^t G(t-t') \frac{d\mathbf{W}}{dt'} dt' + G(t) \mathbf{W}(0^-) \right], \quad (31)$$

$$\mathbf{W}(t) = \mathbf{U}(t) - \mathbf{u}^\infty(\mathbf{X}, t) - \frac{a^2}{6(1+2\hat{\lambda})} \nabla^2 \mathbf{u}^\infty \Big|_{X(t)}. \quad (32)$$

As in Ref. 8, (31) is valid when the particle Reynolds number  $Re_p = \rho|U - u_0|a/\mu$  is small, where  $u_0$  and  $|U - u_0|$  represent the velocity scales for the imposed flow  $\mathbf{u}^\infty$  and the perturbed flow  $\mathbf{u}'$ , respectively. In addition, the inertial terms  $\rho[\mathbf{u}' \cdot \nabla \mathbf{u}^\infty + \mathbf{u}^\infty \cdot \nabla \mathbf{u}']$  are negligible compared to the viscous term  $\mu \nabla^2 \mathbf{u}'$  in the fluid momentum equation provided that the shear Reynolds number  $Re_{shear} = (a^2/\nu)(u_0/L)$  is small in the length scale  $L$  over which  $\nabla \mathbf{u}^\infty$  varies. Also given that  $m_f D\mathbf{u}^\infty/Dt$  differs than  $m_f \partial \mathbf{u}^\infty/\partial t$  by  $m_f \mathbf{u}^\infty \cdot \nabla \mathbf{u}^\infty$ , this difference, because of  $Re_{shear} \ll 1$ , is  $O(a^2 u_0/\nu L)$  compared to the Stokes drag term of  $O(\mu u_0 a)$  and is hence small. Therefore,  $D\mathbf{u}^\infty/Dt$  under this condition can be approximated as  $\partial \mathbf{u}^\infty/\partial t$ . In Sec. V, we will illustrate particle dynamics by solving (31) under  $Re_p \ll 1$  and  $Re_{shear} \ll 1$ .

#### IV. MODIFIED FAXEN TORQUE LAW AND EQUATION OF ANGULAR DYNAMICS FOR A SLIP SPHERE

Similar to Sec. III, we evaluate the torque using (19) with the following rotation resistance density matrix (which is derived in Appendix B):

$$\mathcal{R}^R = \frac{-3\mu}{a} \left[ \frac{1 + \alpha + \alpha^2/3}{(1 + \alpha)(1 + 3\hat{\lambda}) + \hat{\lambda}\alpha^2} \right] \mathbf{I}. \quad (33)$$

Using (21) with  $\hat{\mathbf{u}}^\infty = \boldsymbol{\Omega} \times \mathbf{x} - \mathbf{u}^\infty$  because of no contributions from  $\mathbf{U}$ , the  $\hat{\mathbf{u}}^\infty$  term in (19) contributes to a torque of

$$-8\pi a^3 \mu \left[ \frac{1 + \alpha + \alpha^2/3}{(1 + \alpha)(1 + 3\hat{\lambda}) + \hat{\lambda}\alpha^2} \right] \left( \boldsymbol{\Omega} - \frac{1}{2} (\nabla \times \mathbf{u}^\infty)_0 \right). \quad (34)$$

Using (22) to evaluate the slip term in (19), we find that the only contribution comes from  $(1/2)\mathbf{xx} : \nabla \nabla \boldsymbol{\sigma}^\infty(0)$  in (22). It can also be shown that the integral  $\int_{S_p} \mathbf{x} \times \mathbf{n} \cdot (1/2)\mathbf{xx} : \nabla \nabla \boldsymbol{\sigma}^\infty(0) \cdot \mathbf{n} dS$  is identically zero (see Appendix C for the detailed derivation). The result will end up with a form like  $\nabla \times (\nabla \cdot \boldsymbol{\sigma}^\infty)_0 = \nabla \times (-i\omega \rho \mathbf{u}^\infty)_0$ , giving

$$-\frac{4}{5} \lambda \pi a^5 \left[ \frac{1 + \alpha + \alpha^2/3}{(1 + \alpha)(1 + 3\hat{\lambda}) + \hat{\lambda}\alpha^2} \right] (\nabla \times (-i\omega \rho \mathbf{u}^\infty))_0. \quad (35)$$

Combining (34) and (35) yields the Faxen second law for the torque,

$$\frac{\mathcal{T}}{-8\pi\mu a^3} = \left[ \frac{1 + \alpha + \alpha^2/3}{(1 + \alpha)(1 + 3\hat{\lambda}) + \hat{\lambda}\alpha^2} \right] \left\{ \left( \boldsymbol{\Omega} - \frac{1}{2} (\nabla \times \mathbf{u}^\infty)_0 \right) + \frac{\hat{\lambda}}{10} \alpha^2 (\nabla \times \mathbf{u}^\infty)_0 \right\}. \quad (36)$$

Equation (36) basically agrees with the torque expression obtained previously by Felderhof.<sup>26</sup> However, here, the surface integral of the background flow velocity in his expression is now made more explicit in terms of the local vorticity of the imposed flow,  $(\nabla \times \mathbf{u}^\infty)_0$ . In steady motion with  $\alpha = 0$ , it recovers the result obtained by Ref. 43. Equation (36) without imposed flows (i.e.,  $\mathbf{u}^\infty = 0$ ) also reduces to the torque on a slip sphere undergoing rotary oscillations.<sup>22</sup> When there is an unsteady imposed flow, however, an additional inertia torque—the last term in (36)—will arise from slip through the local flow vorticity. This contribution is new because it is absent in the no-slip situation.

To derive the corresponding time-dependent form of (36), we let  $\alpha^2 = s$  to rewrite (36) as

$$\frac{\mathcal{T}(s)}{-8\pi a^3 \mu} = \frac{1}{1 + 3\hat{\lambda}} \left[ \frac{1}{s} + Q(s) \right] \left\{ s \tilde{\boldsymbol{\Omega}}(s) + \frac{\hat{\lambda}}{10} s^2 (\nabla \times \mathbf{u}^\infty(s))_0 \right\}. \quad (37)$$

In the above,  $\tilde{\boldsymbol{\Omega}}(s) = \boldsymbol{\Omega}(s) - (1/2)(\nabla \times \mathbf{u}^\infty(s))_0$ , and  $Q(s)$ , the Laplace transform of the yet-determined memory kernel, is given by



$$\begin{aligned}
 Q(s) &= \frac{1}{3\hat{\lambda}(s + \beta^{-1}s^{1/2} + \beta^{-1})} \\
 &= \frac{1}{3\hat{\lambda}(b_2 - b_1)} \left[ \frac{1}{(s^{1/2} + b_1)} - \frac{1}{(s^{1/2} + b_2)} \right], \quad (38)
 \end{aligned}$$

with

$$b_1 = \frac{1 - \sqrt{1 - 4\beta}}{2\beta}, \quad b_2 = \frac{1 + \sqrt{1 - 4\beta}}{2\beta}.$$

Using the following inverse Laplace transform in terms of the dimensionless time  $\tau = t/t_v$ :

$$\mathcal{L}^{-1} \left\{ \frac{1}{s^{1/2} + b} \right\} = \frac{1}{\sqrt{\pi\tau}} - b \exp(b^2\tau) \operatorname{erfc}(b\sqrt{\tau}), \quad (39)$$

we can determine the memory kernel for  $\hat{\lambda} \neq 1$  as

$$\begin{aligned}
 Q(\tau) &= \frac{1}{3\hat{\lambda}(b_2 - b_1)} \left[ -b_1 \exp(b_1^2\tau) \operatorname{erfc}(b_1\sqrt{\tau}) \right. \\
 &\quad \left. + b_2 \exp(b_2^2\tau) \operatorname{erfc}(b_2\sqrt{\tau}) \right], \quad (40)
 \end{aligned}$$

in accordance with the memory integral reported previously.<sup>22-24</sup>

Next, we take an inverse Laplace transform for (37) with

$$\mathcal{L}^{-1} \{ Q(s) s \tilde{\Omega}(s) \} = \int_0^t Q(t-t') \frac{d\tilde{\Omega}(t')}{dt'} dt + Q(t) \tilde{\Omega}(t=0), \quad (41)$$

$$\begin{aligned}
 \mathcal{L}^{-1} \{ s Q(s) s (\nabla \times \mathbf{u}^\infty(s))_0 \} \\
 = \frac{d}{dt} \int_0^t Q(t-t') \frac{d}{dt'} (\nabla \times \mathbf{u}^\infty(t'))_0 dt'. \quad (42)
 \end{aligned}$$

We can then convert (37) into the following form:

$$\begin{aligned}
 \frac{\mathcal{T}(t)}{-8\pi a^3 \mu} &= \left[ \boldsymbol{\Omega}(t) - \frac{1}{2} (\nabla \times \mathbf{u}^\infty(t))_0 \right] \\
 &\quad + \int_0^t Q(t-t') \frac{d}{dt'} \left[ \boldsymbol{\Omega}(t') - \frac{1}{2} (\nabla \times \mathbf{u}^\infty(t'))_0 \right] dt' \\
 &\quad + Q(t) \left[ \boldsymbol{\Omega}(t=0^-) - \frac{1}{2} (\nabla \times \mathbf{u}^\infty(t=0^-))_0 \right] \\
 &\quad + \frac{\hat{\lambda}}{10} \frac{d}{dt} \int_0^t Q(t-t') \frac{d}{dt'} (\nabla \times \mathbf{u}^\infty(t'))_0 dt'. \quad (43)
 \end{aligned}$$

Equation (43) agrees with the time-dependent torque reported previously,<sup>23,24</sup> except that the surface integral of the fluid angular momentum within the sphere in the latter is now expanded as the Faxen terms. In the absence of slip, (43) reduces to the Basset torque found previously<sup>48,51-53</sup> with the memory kernel

$$Q_B(t) = \frac{1}{3} \left\{ \frac{1}{\sqrt{\pi}} \left( \frac{t_v}{t} \right)^{1/2} - \exp\left( \frac{t}{t_v} \right) \operatorname{erfc} \left[ \left( \frac{t}{t_v} \right)^{1/2} \right] \right\}. \quad (44)$$

Much like the situation occurring to a nearly spherical no-slip particle<sup>40,41</sup> or to a spherical drop,<sup>31,32</sup> (44) is made of a singular Basset part and a regular non-Basset part. Because of the Basset part,  $Q_B$  will diverge as  $t^{-1/2}$  as  $t \rightarrow 0$ . However, for long times, the Basset part will be killed by the non-Basset part, making  $Q_B = (1/6\sqrt{\pi})(t_v/t)^{3/2} + O((t_v/t)^{5/2})$  to decay as  $t^{-3/2}$ .

For the slip case, on the contrary,  $Q$  given by (40) behaves rather differently, as can be seen in Fig. 3 that plots  $Q$  against  $t$ . Figure 3 is essentially equivalent to looking at the torque response when a slip sphere rotates suddenly from rest to a constant angular velocity. Compared to the no-slip kernel  $Q_B$  given by (44), the first difference is that  $Q$  is finite at  $t = 0$ , as can be revealed from its short-time behavior,

$$Q(t) = \frac{1}{3\hat{\lambda}} \left[ 1 - \frac{2}{\sqrt{\pi}} \left( \frac{t}{\beta^2 t_v} \right)^{1/2} \right] + O(t/t_v). \quad (45)$$

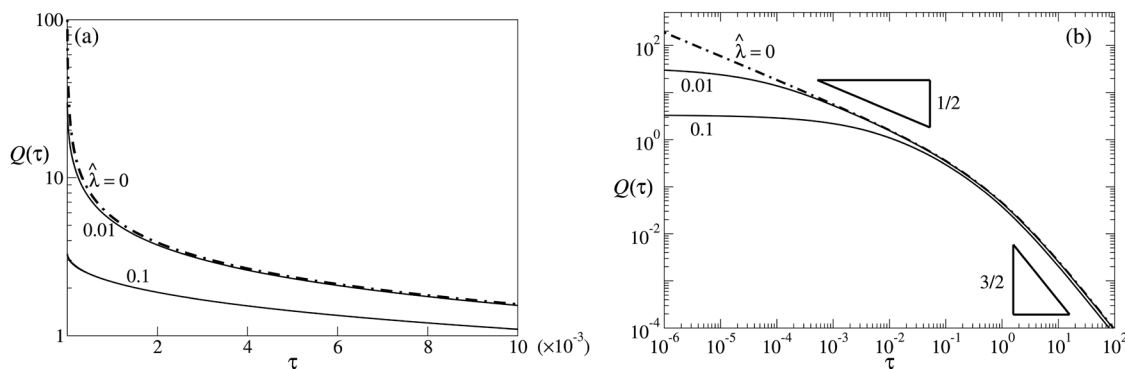


**FIG. 3.** (a) Temporal evolution of the non-Basset memory kernel  $Q$  given by (40) for the unsteady rotation of weak slip spheres with  $\hat{\lambda} \ll 1$ , displaying a behavior similar to  $G$  for unsteady translation shown in Fig. 2(a). (b) is the corresponding log-log plot. These results are plotted against time  $\tau = t/t_v$ , scaled by the viscous time  $t_v$ . At short times,  $Q$  approaches a constant plateau as time  $\tau \rightarrow 0$ , in contrast to the  $\tau^{-1/2}$  Basset decay for the no-slip case. A transition from the former to the latter takes place at around their crossover time  $\tau \sim \hat{\lambda}^2$  due to the slip-stick transition. At sufficiently long times,  $Q$  decays as  $\tau^{-3/2}$ , regardless of the amount of slip.

Similar to  $G$  given by (27),  $Q$  displays a constant plateau  $1/3\hat{\lambda}$  as  $t \rightarrow 0$ , which is again attributed to the constant shear stress that resulted from strong slip effects.<sup>22</sup> Because of (45),  $Q$  will decay with time less rapidly compared to  $Q_B$ , as shown in Fig. 3(a). However, unlike  $G$  for the translational problem,  $Q$  will vanish in the bubble  $\hat{\lambda} \rightarrow \infty$  limit because a full slip particle will not rotate at all due to zero shear stress on the particle. For  $\hat{\lambda} \ll 1$ , (45) behaves as

$$Q(t) \approx \frac{1}{3\hat{\lambda}} \left[ 1 - \frac{2}{\sqrt{\pi}} \left( \frac{t}{\hat{\lambda}^2 t_v} \right)^{1/2} \right] + O(t/\hat{\lambda}^2 t_v). \quad (46)$$

Hence,  $Q$  in this case will start to decrease with time at around the slip-stick transition time  $t_\lambda = \hat{\lambda}^2 t_v = \lambda^2/\nu$ , similar to  $G$  given by (30) for the translational problem. However, for long times where vorticity has already been diffused to a distance  $\delta \sim (\nu t)^{1/2}$  much larger than the slip length  $\hat{\lambda}$ ,  $Q = (1/6\sqrt{\pi})(t_v/t)^{3/2} + O((t_v/t)^{5/2})$  from (40) becomes irrelevant of  $\hat{\lambda}$  to decay with time as  $t^{-3/2}$ , recovering the long-time behavior of  $Q_B$ , as shown in Fig. 3(b). As will be demonstrated in Sec. V C, the differences between  $Q$  and  $Q_B$  mentioned above can be best revealed from the angular response of a slip particle when it is subjected to a torque impulse.

To determine the angular dynamics of a slip sphere, we need to solve the following equation of motion by including the hydrodynamic torque (43):

$$I_p \frac{d\boldsymbol{\Omega}}{dt} = \mathcal{T}_{ex} + (1/2)I_f \nabla \times \frac{D\mathbf{u}^\infty}{Dt} \Big|_0 + \mathcal{T}(t), \quad (47)$$

where  $I_p = (2/5)m_p a^2$  and  $I_f = (\rho/\rho_p)I_p$  represent the rotational inertias for the particle and the surrounding fluid, respectively, and  $\mathcal{T}_{ex}$  is the applied torque. Similar to (31), (36) holds when the particle Reynolds number  $Re_p = a|a\boldsymbol{\Omega} - \mathbf{u}_0|/\nu$  is small. The second term on the right-hand side of (36) accounts for the fluid angular acceleration around the sphere  $\rho \int_{\gamma_p} \mathbf{x} \times D\mathbf{u}^\infty/Dt d\mathcal{V}$  with an expansion of  $D\mathbf{u}^\infty/Dt$  at the particle's center.<sup>54</sup> This term can be approximated as  $(1/2)I_f \partial(\nabla \times \mathbf{u}^\infty)_0/\partial t$  by further assuming that the shear Reynolds number  $Re_{shear} = (a^2/\nu)(u_0/L)$  is small.

## V. IMPACTS OF SLIP ON UNSTEADY PARTICLE MOTIONS: ATYPICAL NON-BASSET DYNAMICS

Given the non-Basset memory kernels (27) and (40), in this section, we will solve the modified equations of motion (31) and (47) with specific examples to illustrate dynamic distinctions of a slip particle to a no-slip particle, as well as to a bubble.

### A. Transient sedimentation

We first consider the transient sedimentation of a slip particle under the gravity force  $F_g = (m_p - m_f)g$  (with  $g$  being gravitational acceleration). Assume that the particle is initially at rest,  $U(t = 0^-) = 0$ . The equation of particle motion(31) is reduced to

$$\left( m_p + \frac{1}{2} m_f \right) \frac{dU}{dt} = F_g - 6\pi\mu a \Lambda U - 6\pi\mu a \Lambda^2 \int_0^t G(t-t') \frac{dU}{dt'} dt'. \quad (48)$$

We rescale the particle velocity as  $V = U/U_0$  with the no-slip Stokes terminal velocity  $U_0 = F_g/6\pi\mu a$  and time  $\tau = t/t_v$  with the viscous relaxation time  $t_v = a^2/\nu$ . Using the above, (48) can be non-dimensionalized as

$$M \frac{dV}{d\tau} = 1 - \Lambda V - \Lambda^2 \int_0^\tau G(\tau - \tau') \frac{dV}{d\tau'} d\tau', \quad (49)$$

where  $M = (2\rho_p/\rho + 1)/9$  is the effective particle mass. Here, the particle Reynolds number is  $Re_p = U_0 a/\nu = t_v/t_0$ , which is also the ratio of  $t_v = a^2/\nu$  to the characteristic traveling time  $t_0 = a/U_0$ . Effects of particle inertia to viscous damping is reflected by the Stokes number  $St = t_{damp}/t_0$  in terms of the ratio of the viscous damping time  $t_{damp} = a^2\rho_p/\mu$  to  $t_0 = a/U_0$ . Take a micrometer-sized aerosol particle (of  $a \sim \mu\text{m}$ ) falling in air as an example. With typical values  $\rho_p \approx 2 \text{ g/cm}^3$ ,  $\rho \approx 10^{-3} \text{ g/cm}^3$ , and  $\mu \approx 2 \times 10^{-4} \text{ g/cm-s}$ , the particle's terminal velocity is  $U_0 = (2a^2/9\mu)(\rho_p - \rho)g \sim 2 \times 10^{-2} \text{ cm/s}$ . Hence, both  $Re_p \sim 10^{-5}$  and  $St \sim 2 \times 10^{-2}$  are pretty small, to which (49) can be applied.

The solution to (49) can be determined analytically using the Laplace transform as follows: We first take Laplace transform for (49) with  $V(\tau = 0^-) = 0$ , which yields

$$V(s) = \frac{1}{\beta M s} \left[ \frac{\beta s^{1/2} + 1}{D_1(s^{1/2})} \right], \quad (50)$$

with the characteristic equation

$$D_1(z) = z^3 + \beta^{-1} z^2 + M^{-1}(\Lambda + \Lambda^2 \beta^{-1})z + \Lambda(\beta M)^{-1}. \quad (51)$$

To invert (50), we recast it into the following form:

$$V(s) = \frac{1}{\beta M} \left[ \frac{A_1}{s(s^{1/2} + \gamma_1)} + \frac{A_2}{s(s^{1/2} + \gamma_2)} + \frac{A_3}{s(s^{1/2} + \gamma_3)} \right], \quad (52)$$

where  $\gamma_1$ ,  $\gamma_2$ , and  $\gamma_3$  are the roots of  $D_1(-z) = 0$  from (51). The coefficients  $A_1$ ,  $A_2$ , and  $A_3$  are determined as

$$A_1 = \frac{1 - \beta\gamma_1}{(\gamma_1 - \gamma_2)(\gamma_1 - \gamma_3)}, \quad A_2 = \frac{1 - \beta\gamma_2}{(\gamma_2 - \gamma_1)(\gamma_2 - \gamma_3)},$$

$$A_3 = \frac{1 - \beta\gamma_3}{(\gamma_3 - \gamma_1)(\gamma_3 - \gamma_2)}.$$

Equation (52) allows us to make its inversion with

$$\mathcal{L}^{-1} \left\{ \frac{1}{s(s^{1/2} + \gamma)} \right\} = \gamma^{-1} (1 - \exp(\gamma^2 \tau) \text{erfc}(\gamma\sqrt{\tau})), \quad (53)$$

yielding an analytical solution for  $V(\tau)$ ,

$$V(\tau) = \frac{1}{\beta M} \sum_{n=1}^3 A_n \gamma_n^{-1} [1 - \exp(\gamma_n^2 \tau) \text{erfc}(\gamma_n \sqrt{\tau})]. \quad (54)$$

Using (54), we plot  $V$  against  $\tau$  for various values of  $\hat{\lambda}$ , as shown in Fig. 4(a). For a given value of  $\hat{\lambda}$ ,  $V$  typically grows rapidly with time at early times and then gradually slows down toward the Stokes

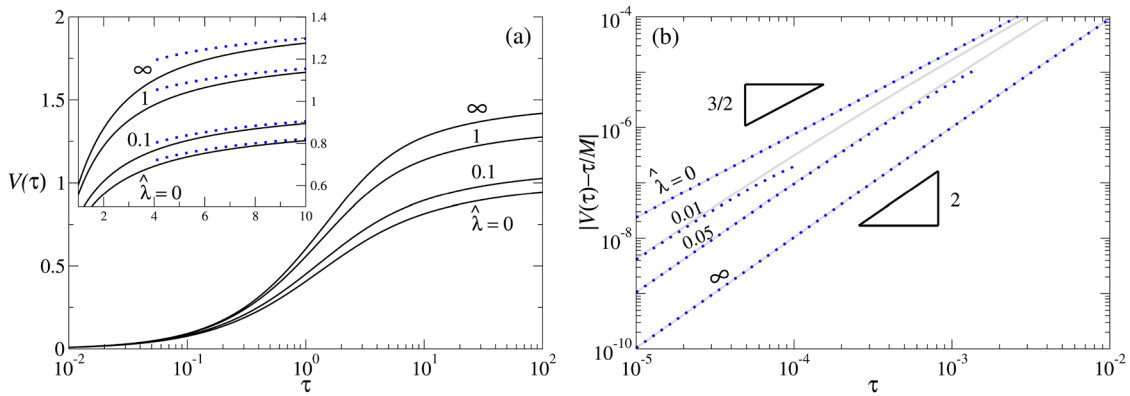


**FIG. 4.** Effects of slip on the transient velocity response of a settling particle with  $M = 1$ . (a) Plot of the particle falling speed  $V$  described by (54) against  $\tau$ . It reveals that  $V$  with slip accelerates faster than that without slip (D4) and that increasing slip makes  $V$  even faster. The inset shows the corresponding curves in the long-time regime with dotted lines representing the asymptotic results for the slip case (57) and the no-slip case (D7). (b) The short-time plot for the velocity correction to the constant acceleration  $\tau/M$ , showing that the correction for the slip case first enters as  $O(\tau^2)$  in contrast to  $O(\tau^{3/2})$  for the no-slip case. Short-time asymptotic results (dotted lines) are also plotted for the slip case (55) and the no-slip case (D5). Note that at some later time, the velocity correction for a weak slip particle will undergo a slip–stick transition, as shown for  $\hat{\lambda} = 0.01$  and  $0.05$ . In the bubble  $\hat{\lambda} \rightarrow \infty$  limit, on the contrary, the trend still keeps as  $O(\tau^2)$  because of the lack of the slip–stick transition.

terminal velocity at late times. Increasing  $\hat{\lambda}$  makes  $V$  faster because of drag reduction by slip effects. However, this speedup effect will become saturated when further increasing  $\hat{\lambda}$  toward the bubble limit  $\hat{\lambda} \rightarrow \infty$  whose terminal velocity is 1.5 times faster than that of the no-slip case. To gain more insight into how slip effects modify the characteristics of the particle motion, in the following, we carry out asymptotic analyses for both short-time and long-time regimes. The results are found to well capture the trends calculated from (54), as also shown in Fig. 4(a).

For short times  $\tau \ll 1$ , the behavior can be determined much easier by taking a large  $s$  expansion for (50),

$$V(s) = \frac{1}{M} \left[ \frac{1}{s^2} - \frac{1}{s^3} \frac{\Lambda + \beta^{-1} \Lambda^2}{M} + \frac{1}{s^{7/2}} \frac{\beta^{-2} \Lambda^2}{M} \right] + O(s^{-4}).$$

The corresponding inversion is then

$$V(\tau) = \frac{\tau}{M} - \left( \frac{\Lambda + \beta^{-1} \Lambda^2}{2M^2} \right) \tau^2 + \frac{8}{15\sqrt{\pi}} \frac{\beta^{-2} \Lambda^2}{M^2} \tau^{5/2} + O(\tau^3), \quad (55)$$

which well describes the short-term behavior of (54), as shown in Fig. 4(b). As indicated by (55), the leading contribution is constant acceleration  $\tau/M$ , corresponding to the free-fall speed  $U_M = (F_g/(m_p + m/2))t$  as expected. The correction due to viscous retardation first appears as  $O(\tau^2)$ . This is markedly different from  $O(\tau^{3/2})$  found for the no-slip case<sup>55</sup> (see also Appendix D 1) and for the drop case,<sup>32</sup> as clearly shown in Fig. 4(b). A more heuristic way to see such an  $O(\tau^2)$  correction can be realized by solving (49) asymptotically with  $V = V^{(0)} + V^{(1)} + \dots$  in which the correction velocity  $V^{(1)}$  to the constant acceleration  $V^{(0)} = \tau/M$  can be determined by solving the following equation:

$$M \frac{dV^{(1)}}{d\tau} = -\Lambda V^{(0)} + \Lambda^2 \frac{dV^{(0)}}{d\tau} \int_0^\tau G(\tau - \tau') d\tau', \quad (56)$$

wherein  $G$  given by (27) is taken in a small  $\tau$  expansion:  $G = \beta^{-1} \left( 1 - (2/\sqrt{\pi}) [\tau/\beta^2]^{1/2} \right) + O(\tau^{3/2})$ . As indicated by (56), the  $O(\tau^2)$  velocity correction comes from two contributions: (i) the instantaneous Stokes drag at speed  $V^{(0)}$  (the  $\Lambda$  term) and (ii) the linear acceleration by the history force due to  $V^{(0)}(\tau)$  (the  $\Lambda^2$  term). Because  $G(\tau \ll 1) \approx \beta^{-1} = 3 + \hat{\lambda}^{-1}$  here, the history force contribution will dominate when the slip length  $\hat{\lambda}$  is small. As also indicated by (55), for small  $\hat{\lambda}$ , the constant acceleration will start to be slowed down by the history force in a time scale of  $\tau \sim O(\hat{\lambda}M)$  or  $t \sim (\lambda a/\nu)M$ , which is a reminiscent of the slip–stick transition. Compared to the no-slip case where  $V^{(1)}$  occurs at  $O(\tau^{3/2})$ , this characteristic change in the particle motion is attributed to different natures between non-Basset force and Basset force. In the slip case,  $V^{(1)}$  is driven by a non-Basset force that gives rise to a dominant slip force plateau  $F_\lambda \sim \mu U_M(t) a^2/\lambda \propto t$  at short times, resulting from the shear stress  $\mu U_M(t)/\lambda$  across the slip length  $\lambda$  much thicker than the particle size  $a$ .<sup>49</sup> The velocity acceleration by this force thus leads to  $V^{(1)} \propto t^2$ . In contrast, in the no-slip case,  $V^{(1)}$  is accelerated by a Basset force  $F_B \sim \mu U_M(t) a^2/\delta(t) \propto t^{1/2}$  due to the shear stress across the vorticity diffuse layer of thickness  $\delta(t) \sim (\nu t)^{1/2}$  and hence varies as  $t^{3/2}$  (see Appendix D 1).

It is worth mentioning that the same  $O(\tau^2)$  velocity correction also occurs to a rising of a spherical bubble whose memory kernel  $G_{bubble}$  also takes the form (27) with  $\hat{\lambda} \rightarrow \infty$ . In this case, since  $G$  becomes saturated as  $\hat{\lambda} \rightarrow \infty$  and  $G_{bubble}(\tau \ll 1) = 3 - (2/\sqrt{\pi}) \tau^{1/2} + O(\tau^{3/2})$  is reduced to a constant irrelevant of  $\hat{\lambda}$  as  $\tau \rightarrow 0$ , both the Stokes drag and the history force in (56) become comparable. Consequently, from (55), the time scale to see a slowdown of the constant acceleration is  $\tau \sim O(M)$  or  $t \sim (a^2/\nu)M$ , longer by a factor  $\hat{\lambda}^{-1}$  compared to  $\tau \sim O(\hat{\lambda}M)$  or  $t \sim (\lambda a/\nu)M$  for the weak slip case discussed above. For a nearly spherical no-slip particle or a spherical liquid drop, while a non-Basset kernel can emerge, the total memory kernel still contains the Basset kernel that diverges as  $\tau^{-1/2}$  as  $\tau \rightarrow 0$ .<sup>31,32,40,41</sup>

Hence, the short-time particle dynamics in these cases will be nearly the same as that of a no-slip spherical particle, predominated by the singular Basset kernel. This explains why a similar  $O(\tau^{3/2})$  velocity correction is also found in the transient settling/rising of a spherical drop.<sup>32</sup>

In fact, the dynamic distinction between a weak slip particle and a full slip bubble can be seen in the detailed behaviors of their short-time responses. As shown in Fig. 4(b), at some later time, a weak slip particle with  $\hat{\lambda} \ll 1$  will start to depart from  $O(\tau^{3/2})$  and gradually approach toward the no-slip case due to the second order correction  $V^{(2)}$ . In this case, (55) shows that  $V^{(2)}$  occurs at  $O(\tau^{5/2})$  with magnitude  $\beta^{-2}\Lambda^{-2}/M \sim \hat{\lambda}^{-2}/M$  purely due to the history term. Since the corresponding first order correction  $V^{(1)} \sim (\hat{\lambda}^{-1}/M)\tau^2$  is also dominated by the history term, its transition to the  $O(\tau^{5/2})$  correction will take place at  $\tau \sim \hat{\lambda}^2$  or  $t \sim \lambda^2/\nu$  around the slip-stick transition point, as seen in the curves of  $\hat{\lambda} = 0.01$  and  $0.05$  in Fig. 4(b). For a full slip bubble with  $\hat{\lambda} \rightarrow \infty$ , on the contrary, such an  $O(\tau^{5/2})$  correction will take place at a time scale much longer than the weak slip case, meaning that one will have to wait an even longer time to see a change in the velocity correction to a different trend other than  $O(\tau^2)$ . This explains why the velocity correction in this case is kept virtually at  $O(\tau^2)$  throughout the short-time regime, as displayed in Fig. 4(b).

For long times  $\tau \gg 1$ , (50) in a small  $s$  expansion is

$$V(s) = \frac{1}{\Lambda s} - \frac{1}{s^{1/2}} + \dots,$$

hence leading to

$$V(\tau) = \frac{1}{\Lambda} - \frac{1}{\sqrt{\pi\tau}} + \dots, \quad (57)$$

which fairly captures the long-term behavior of (54), as shown in the inset of Fig. 4(a). In the dimensional form, (57) is essentially the Stokes terminal velocity  $U_s = F_g/6\pi\mu a\Lambda = U_0/\Lambda$  plus the prior Basset  $t^{-1/2}$  attenuation regardless of the amount of slip.

To explain (57), we anticipate that the long-term behavior of the particle velocity takes the form of  $V = V_\infty^{(0)} + V_\infty^{(1)} + \dots$ , where  $V_\infty^{(1)} = U_\infty^{(1)}/U_0$  being the first correction to the terminal velocity  $V_\infty^{(0)} = 1/\Lambda$  can be sought by solving (49) asymptotically. Given  $G(\tau) = 1/(\pi\tau)^{1/2} + O(\tau^{-3/2})$  for  $\tau \gg 1$ , to correctly capture the history force asymptotically, we first extract the Basset kernel  $G_B(\tau) = 1/(\pi\tau)^{1/2}$  from  $G$  to rewrite the memory integral as

$$\int_0^\tau G(\tau - \tau') \frac{dV}{d\tau'} d\tau' = \int_0^\tau [G(\tau - \tau') - G_B(\tau - \tau')] \frac{dV}{d\tau'} d\tau' + \int_0^\tau G_B(\tau - \tau') \frac{dV}{d\tau'} d\tau'. \quad (58)$$

In (58), the first term on the right is  $O(\tau^{-3/2})$  or smaller. Next, following Ref. 21, we re-express the second term as

$$\frac{1}{\sqrt{\pi}} \int_0^\tau \frac{1}{\sqrt{\tau - \tau'}} \frac{dV}{d\tau'} d\tau' = \frac{1}{\sqrt{\pi}} \frac{d}{d\tau} \int_0^\tau \frac{1}{\sqrt{\tau - \tau'}} V(\tau') d\tau' - \frac{1}{\sqrt{\pi}} \frac{V(0)}{\sqrt{\tau}}. \quad (59)$$

Because  $V(0) = 0$  here, only the first term of the above contributes and appears as  $O(\tau^{-1/2})$ . Finally, after substituting  $V = V_\infty^{(0)} + V_\infty^{(1)}$  into (49) with the approximate memory integral (59), we arrive at the following equation for  $V_\infty^{(1)}$ :

$$M \frac{dV_\infty^{(1)}}{d\tau} = -\Lambda V_\infty^{(1)} - \Lambda^2 \frac{V_\infty^{(0)}}{\sqrt{\pi\tau}}. \quad (60)$$

As indicated by (60), as  $\tau \rightarrow \infty$ , the inertial term on the left will be damped out, making  $V_\infty^{(1)}$  approach  $-\Lambda V_\infty^{(0)}/(\pi\tau)^{1/2} = -1/(\pi\tau)^{1/2}$ . In the dimensional form, this is essentially the result by balancing the Stokes drag  $-6\pi\mu a\Lambda U_\infty^{(1)}$  to the Basset force  $-6\pi\Lambda\mu U_s a^2/\delta(t)$  within the vorticity diffuse layer  $\delta(t) = (\pi\nu t)^{1/2}$ . In other words, for long times, because vorticity has already diffused to a distance much larger than the slip length  $\lambda$ , slip does nothing but reduce the drag coefficient without changing the viscous relaxation characteristics. This also explains why  $V_\infty^{(1)}$  appears independent of  $\lambda$ .

## B. Translational response to a suddenly applied stream

In the second case, we consider the situation with flow to look at how a slip particle responds. Here, the fluid is initially stationary and suddenly subject to a non-uniform flow:  $\mathbf{u}^\infty(\mathbf{x}, t) = \mathbf{v}^\infty(\mathbf{x})H(t)$  with the Heaviside step function  $H(t) = 0$  for  $t = 0$ ; otherwise 1 for  $t > 0$ . The particle is initially moving at a constant velocity  $U_i$  before the flow is applied. At the moment  $t = 0^+$  when the flow is applied, the particle velocity is suddenly changed to  $U(t = 0^+) = U_{start}$  due to the instantaneous advection by the imposed flow or to perturbations. Let  $\mathbf{v}^\infty(\mathbf{X}) = v^\infty|_0$  at the particle position  $\mathbf{X}$  in the direction of  $U_i$ . The particle motion governed by (28) in this case takes the form

$$\left(m_p + \frac{1}{2}m_f\right) \frac{dU}{dt} = \left(m_p + \frac{1}{2}m_f\right) (U_{start} - U_i) \frac{dH}{dt} + m_f \left[ v^\infty|_0 + \frac{1}{2} \left[ 1 + \frac{a^2}{10} \nabla^2 \right] v^\infty|_0 \right] \frac{dH}{dt} - 6\pi\mu a \mathcal{U}(t), \quad (61)$$

where

$$\mathcal{U}(t) = \Lambda U(t) - \Lambda \left[ 1 + \frac{a^2}{6(1+2\hat{\lambda})} \nabla^2 \right] v^\infty|_0 H(t) + \Lambda^2 \left\{ \int_0^t G(t-t') \frac{dU}{dt'} dt' - G(t) \left[ 1 + \frac{a^2}{6(1+2\hat{\lambda})} \nabla^2 \right] v^\infty|_0 + G(t) U_i \right\}. \quad (62)$$

The particle Reynolds number in this case is  $Re_p = \Delta U a/\nu$  in terms of the relative velocity  $\Delta U = |U_i - v^\infty|_0$ . For a micrometer-sized particle in an aqueous solution (of  $\nu \approx 10^{-2}$  cm<sup>2</sup>/s),  $\Delta U$  has to be much smaller than 10<sup>2</sup> cm/s to ensure  $Re_p \ll 1$  under which (61) can be applied. This requirement can usually be fulfilled in practice. The shear Reynolds number  $Re_{shear} = (a^2/\nu) (v^\infty|_0/L) = Re_p (v^\infty|_0/\Delta U) (a/L)$  also needs to be small. Since both  $Re_p$  and  $a/L$  ( $< 10^{-2}$ ) are

typically small,  $Re_{shear}$  is normally even smaller than unity unless  $v^\infty|_0$  is much larger than  $\Delta U$ .

Rescaling (61) with  $V = U/v^\infty|_0$  and  $\tau = t/t_v$ , we rewrite it in the dimensionless form,

$$M \frac{dV}{d\tau} = M(V_{start} - V_i) \frac{dH}{d\tau} + J \frac{dH}{d\tau} - \Lambda V - \Lambda^2 \left[ \int_0^\tau G(\tau - \tau') \frac{dV}{d\tau'} d\tau' + G(\tau) V_i \right] + [\Lambda H(\tau) + \Lambda^2 G(\tau)] \left[ 1 + \frac{k}{6(1 + 2\hat{\lambda})} \right], \quad (63)$$

where  $V_{start} = U_{start}/v^\infty|_0$ ,  $V_i = U_i/v^\infty|_0$ , and  $J = 1/3 + k/90$  is the strength of the impulsive inertial force combining the fluid acceleration and the added mass and  $k = a^2 \nabla^2 v^\infty|_0 / v^\infty|_0$  measures the magnitude of the Faxen correction and is generally small. We remark that a similar equation like (62) or (63) also governs the transient particle motion driven by a force impulse, except that there will be no Faxen terms in that situation.

Taking a Laplace transform for (63) with  $V(\tau = 0^-) = V_i$  gives

$$V(s) = \frac{J'}{sM} \left\{ 1 + \frac{C_1 s^{1/2} + C_0}{D_1 (s^{1/2})} \right\}, \quad (64)$$

where  $J' = MV_{start} + J$  is the effective impulsive inertial force and the coefficients in the numerator are found to be

$$C_1 = (\Lambda + \beta^{-1} \Lambda^2) \chi - \frac{\Lambda^2 V_i}{J' \beta}, \quad C_0 = \Lambda \beta^{-1} \chi, \quad \chi = \frac{1}{J'} \left( 1 + \frac{k}{6(1 + 2\hat{\lambda})} \right) - \frac{1}{M}.$$

Similar to the way to derive (54), an analytical solution can be obtained by taking an inverse Laplace transform for (64),

$$V(\tau) = \frac{J'}{M} \left\{ 1 + \sum_{n=1}^3 B_n \gamma_n^{-1} [1 - \exp(\gamma_n^2 \tau) \text{erfc}(\gamma_n \sqrt{\tau})] \right\}, \quad (65)$$

where the coefficients  $B_1, B_2$ , and  $B_3$  are given as

$$B_1 = \frac{C_0 - C_1 \gamma_1}{(\gamma_1 - \gamma_2)(\gamma_1 - \gamma_3)}, \quad B_2 = \frac{C_0 - C_1 \gamma_2}{(\gamma_2 - \gamma_1)(\gamma_2 - \gamma_3)}, \quad B_3 = \frac{C_0 - C_1 \gamma_3}{(\gamma_3 - \gamma_1)(\gamma_3 - \gamma_2)}.$$

Using (65), we plot  $V$  against  $\tau$ . Figure 5 displays typical responses, showing that  $V$  can vary with  $\tau$  in different manners, sensitive to the initial particle velocity  $V_i$  (before the flow is applied) and the starting particle velocity  $V_{start}$  (at the moment of applying the flow). As shown in Fig. 5(a),  $V$  typically starts with a constant value right after the flow is applied with a given  $V_{start}$  regardless of  $V_i$ . The influences of  $V_i$  enter at later times, making  $V$  vary non-monotonically with time. In particular,  $V$  could undergo a temporary acceleration to display a peak if the flow is applied in the direction against the particle's initial movement,  $V_i < 0$ . At long times, the impacts from  $V_{start}$  and  $V_i$  gradually vanish as  $V$  approaches toward its steady value. Figure 5(b) plots effects of  $V_{start}$  on  $V$  under  $V_i = 0$ . Increasing  $V_{start}$  increases the strength of the effective impulsive force  $J'$  and hence increases  $V$ . For the no-slip case, the responses are also similar to those for the slip case shown above. The differences between these two cases are mainly reflected by their velocity correction behaviors in the short-time regime, as shown in Fig. 6.

To explain various responses shown above, we first inspect the short-time  $\tau \ll 1$  behavior of (64) by taking a large  $s$  expansion,

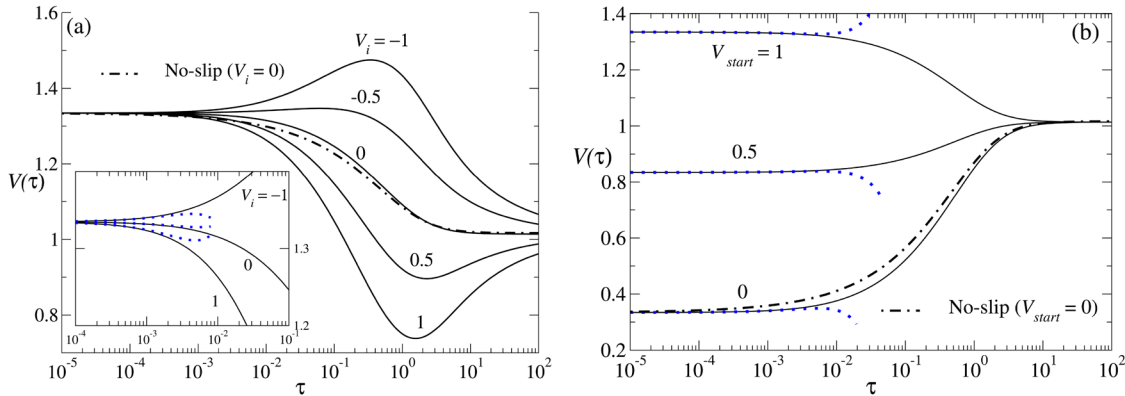


**FIG. 5.** Temporal responses of the translational velocity  $V$  described by (65) for a slip particle in a suddenly applied flow. Short-time asymptotic results (dotted lines) are plotted using (66).  $\hat{\lambda} = 0.1$ ,  $M = 1$ ,  $k = 0.1$ . (a) Plot of  $V$  against  $\tau$  at  $V_{start} = 1$ . At a given particle starting velocity  $V_{start}$ ,  $V$  starts with a constant that is invariant of the particle initial velocity  $V_i$ . The influences of  $V_i$  enter at later times, showing non-monotonic responses with  $\tau$  before approaching toward the steady Stokes velocity that is also independent of  $V_i$ . (b) Effects of  $V_{start}$  on the temporal response of  $V$  at  $V_i = 0$ . Increasing  $V_{start}$  increases the strength of the effective impulsive force  $J'$  and hence increases  $V$  in the beginning of particle motion. The responses for the no-slip case are also similar to those for the slip case shown above. The differences between these two cases are mainly reflected by their velocity correction behaviors in the short-time regime, as shown in Fig. 6.

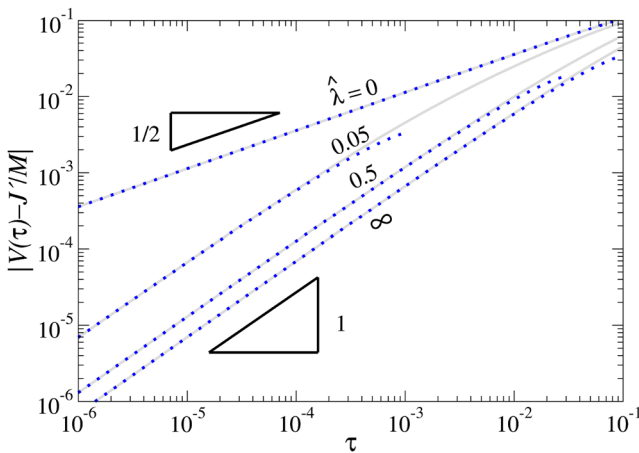


**FIG. 6.** Short-time behavior of the velocity correction  $V - J'/M$  for different values of  $\hat{\lambda}$ .  $V_i = 0$ ,  $V_{start} = 1$ ,  $M = 1$ . The slip case and the no-slip case are plotted using (65) and (D10), respectively. The corresponding short-time asymptotic results (dotted lines) are plotted using (66) and (D13). It can be clearly seen that the velocity correction for the slip case appears as  $O(\tau)$ , distinct from  $O(\tau^{1/2})$  for the no-slip case. Note that the velocity correction for a weak slip particle will gradually change toward the no-slip result at some later time due to the slip-stick transition, as shown in the curves for  $\hat{\lambda} = 0.05$  and  $0.5$ . However, for the bubble  $\hat{\lambda} \rightarrow \infty$  case, because of the lack of the slip-stick transition, the velocity correction always varies as  $O(\tau)$ .

$$V(s) = \frac{J'}{M} \left\{ \frac{1}{s} + \frac{1}{s^2} C_1 + \frac{1}{s^{5/2}} (C_0 - \beta^{-1} C_1) + O(s^{-7/2}) \right\},$$

which leads to

$$V(\tau) = \frac{J'}{M} \left\{ 1 + C_1 \tau + \frac{4}{3\sqrt{\pi}} \beta^{-2} \Lambda^2 (-\chi + J'^{-1} V_i) \tau^{3/2} + O(\tau^{5/2}) \right\}. \quad (66)$$

The leading term is  $V^{(0)} = (J'/M)H(\tau)$  driven by the impulsive inertial force. This term has nothing to do with whether the particle is slip or not. The viscous correction  $V^{(1)}$  first enters at  $O(\tau)$ , making the particle undergo a constant acceleration, as shown in Fig. 6. This  $O(\tau)$  for the slip case is very different from  $O(\tau^{1/2})$  for the no-slip case (whose result is supplemented in Appendix D 2). A closer inspection of the  $O(\tau)$  correction in (66) reveals that the rate of the velocity acceleration is

$$(J'/M)C_1 = \Lambda \left[ 1 + \frac{k}{6(1+2\hat{\lambda})} - V^{(0)} \right] M^{-1} + \beta^{-1} \Lambda^2 \left[ 1 + \frac{k}{6(1+2\hat{\lambda})} - V^{(0)} - V_i \right] M^{-1}, \quad (67)$$

which is caused by the instantaneous Stokes drag [the  $\Lambda$  term with the Faxen correction in (63)] and by the history force [the  $\Lambda^2$  term in (63)]. More precisely, (67) is the result of the small  $\tau$  expansion of (63),

$$M \frac{dV^{(0)}}{d\tau} = J' \frac{dH(\tau)}{d\tau}, \quad (68a)$$

$$M \frac{dV^{(1)}}{d\tau} = \Lambda \left\{ \left[ 1 + \frac{k}{6(1+2\hat{\lambda})} \right] H(\tau) - V^{(0)} \right\} + \Lambda^2 \left\{ G_{\ll}(\tau) \left[ 1 + \frac{k}{6(1+2\hat{\lambda})} \right] - \int_0^\tau G_{\ll}(\tau - \tau') \frac{dV^{(0)}}{d\tau'} d\tau' - G_{\ll}(\tau) V_i \right\}, \quad (68b)$$

wherein the memory kernel  $G_{\ll}(\tau)$  is taken as the short-time constant form:  $G(\tau \ll 1) \approx \beta^{-1} = 3 + \hat{\lambda}^{-1}$ . As indicated by (67) or (68b), if the slip length  $\hat{\lambda}$  is small,  $V^{(1)}$  will be dominated by the history force acceleration  $\hat{\lambda}^{-1} \left[ (1 + k/6(1+2\hat{\lambda})) - V^{(0)} - V_i \right] / M$ —the smaller the  $\hat{\lambda}$ , the greater the acceleration. However, whether  $V^{(1)}$  will grow or decrease with time does not depend on  $\hat{\lambda}$  but on the sign of  $[1 + k/6(1+2\hat{\lambda})] - J'/M - V_i$ , the competition between the steady Stokes velocity  $V_\infty = 1 + k/6(1+2\hat{\lambda})$  [see (70)], and the startup velocity  $V^{(0)} = J'/M$  [see (68a)] together with the initial velocity  $V_i$  of the particle. In other words, for a given imposed flow condition, whether the particle's startup movement is promoted or opposed by the  $O(\tau)$  velocity acceleration at later times will be controlled by the particle's initial velocity  $V_i$ . That is, there exists a critical initial particle velocity  $V_i^* = V_\infty + J'/M$  above (below) which  $V$  will decrease (grow) with time at the early stage of the particle motion. In the special scenario where  $V_i$  is small, the rate of the velocity acceleration (67) is reduced to

$$(J'/M)C_1 \approx (\Lambda + \beta^{-1} \Lambda^2) (V_\infty - V^{(0)}) / M. \quad (69)$$

Hence, the fate of the particle in this case will be determined solely by  $V^{(0)}$  and  $V_\infty$  irrespective of  $V_{start}$  in such a way that (69) determines the initial growth or decline in  $V$  before leveling off toward  $V_\infty$  for long times. When the particle starts its motion with  $V^{(0)} > V_\infty$ ,  $V$  will display a minimum or a maximum otherwise.

Looking at Fig. 6 more closely, we observe that the correction velocity  $V - J'/M$  at some later time will start to depart from the  $O(\tau)$  correction and gradually change toward the no-slip result. In addition, the smaller the  $\hat{\lambda}$ , the earlier the departure will take place. As indicated by (66), such a departure is attributed to the  $O(\tau^{3/2})$  correction. This  $O(\tau^{3/2})$  correction is found to be proportional to  $\beta^{-2} \Lambda^2$  and hence can be identified to come from the history term. When the slip length  $\hat{\lambda}$  is small, in particular, this  $O(\tau^{3/2})$  correction varies as  $\hat{\lambda}^{-2}$ , even more sensitive to  $\hat{\lambda}$ . Therefore, for this weak slip situation, both the  $O(\tau)$  and the  $O(\tau^{3/2})$  corrections are dominated by the history term. Since the  $O(\tau)$  correction varies as  $\hat{\lambda}^{-1}$ , its transition to the  $O(\tau^{3/2})$  correction (which varies as  $\hat{\lambda}^{-2}$ ) will take place at  $\tau \sim \hat{\lambda}^2$  or  $t \sim \lambda^2/\nu$ , which again happens at around the slip-stick transition point.

The long-time  $\tau \gg 1$  response can be determined by taking a small  $s$  expansion for (64),

$$V(s) = \left( 1 + \frac{k}{6(1+2\hat{\lambda})} \right) \frac{1}{s} - \frac{1}{s^{1/2}} \Lambda V_i + \dots,$$

which leads to

$$V(\tau) = \left(1 + \frac{k}{6(1+2\hat{\lambda})}\right) - \frac{1}{\sqrt{\pi\tau}} \Lambda V_i + \dots \quad (70)$$

The leading term is simply the steady Stokes velocity  $V_\infty = 1 + k/6(1+2\hat{\lambda})$  from  $0 = -\Lambda V + \Lambda(1 + k/6(1+2\hat{\lambda}))$  in (63) as  $\tau \rightarrow \infty$ . The correction term occurs at  $O(\tau^{-1/2})$  due to the memory effect that propagates from the initial particle movement before the flow is applied. Similar to the way to derive (63), the correction velocity  $V_\infty^{(1)}$  can be readily found by balancing the Stokes drag to the history force via

$$0 = -\Lambda V_\infty^{(1)} - \Lambda^2 \frac{V_i}{\sqrt{\pi\tau}}. \quad (71)$$

For a gas bubble, its dynamics appear similar to those of a partially slip particle presented above, as the changes are nothing but the coefficients of the equations. The differences between these two cases can only be discerned from the detailed time evolution behaviors of the respective particle velocities. The differences mainly occur in the short-time regime. We first inspect the first order velocity correction at  $O(\tau)$ . As revealed from (67) for the rate of this velocity correction, in the bubble  $\hat{\lambda} \rightarrow \infty$  limit, both the Stokes  $\Lambda$  term and the history  $\beta^{-1}\Lambda^2$  term are comparable. In contrast, the rate for a weak slip particle with  $\hat{\lambda} \ll 1$  is dominated by the history term  $\sim 1/\hat{\lambda}$ .

As for the second order velocity correction  $V^{(2)}$ , (66) reveals that it occurs at  $O(\tau^{3/2})$ . For the weak-slip case,  $V^{(2)}$  appears as  $V^{(2)} \sim \hat{\lambda}^{-2}\tau^{3/2}$ , dominated by the history term. Since  $V^{(1)} \sim \hat{\lambda}^{-1}\tau$  is also dominated by the history term, a transition from  $V^{(1)}$  to  $V^{(2)}$  will take place at  $\tau \sim \hat{\lambda}^2$ , which indicates a slip-stick transition. However, for the bubble case,  $V^{(2)} \sim \tau^{3/2}$  and  $V^{(1)} \sim \tau$  because of the lack of the slip-stick transition. Hence, it will take an even longer time than the weak-slip case to see a transition from  $V^{(1)}$  to  $V^{(2)}$ .

Putting all together, while both slip and bubble cases show  $O(\tau)$  velocity corrections in the very beginning of their movements, they can behave differently at later times. For a weak slip particle, its velocity response will gradually change toward the no-slip result at later times, whereas a full slip bubble remains nearly unchanged in its short-time velocity behavior, as shown in Fig. 6. This distinction in the particle dynamics is mainly due to the fact that there is an inherent slip-stick transition for a weak slip particle but not for a full slip bubble.

### C. Angular response to a torque impulse

To demonstrate non-Basset dynamics due to slip, we examine the angular response of a slip sphere when it is subjected to a torque impulse  $\mathcal{T}_{ex} = L\delta(t)$ . Assume that the sphere is initially at rest, i.e.,  $\Omega(t=0^-) = 0$ . The angular Eq. (47) with the torque (43) in the absence of flows reads

$$I_p \frac{d\Omega}{dt} = L\delta(t) - \frac{8\pi\mu a^3}{(1+3\hat{\lambda})} \Omega(t) - \frac{8\pi\mu a^3}{(1+3\hat{\lambda})} \int_0^t Q(t-t') \frac{d\Omega}{dt'} dt', \quad (72)$$

with the non-Basset memory kernel  $Q$  given by (40). In this case, the impulse accelerates the sphere to start at the angular velocity  $\Omega(t=0) = L/I_p$ . Re-scaling the angular velocity as  $\Gamma = \Omega/\Omega(t=0)$  and time as  $\tau = t/t_v$ , we can write (72) in the dimensionless form as

$$\frac{d\Gamma}{d\tau} = \delta(\tau) - \frac{K}{(1+3\hat{\lambda})} \Gamma - \frac{K}{(1+3\hat{\lambda})} \int_0^\tau Q(\tau-\tau') \frac{d\Gamma}{d\tau'} d\tau', \quad (73)$$

where  $K = 8\pi\rho a^5/I_p = 15\rho/\rho_p$  reflects the fluid-to-particle rotational inertia ratio and  $K/(1+3\hat{\lambda})$  measures the magnitude of the viscous torque relative to the impulse. The particle Reynolds number here can be defined as  $Re_p = \Omega(t=0)a^2/\nu$ . Hence, to ensure the validity of (73) under  $Re_p \ll 1$ ,  $\Omega(t=0)$  cannot exceed the inverse of the viscous relaxation time  $a^2/\nu$ . For a micrometer-sized particle in an aqueous solution (of  $\nu \approx 10^{-2} \text{ cm}^2/\text{s}$ ), (73) is applicable at  $\Omega(t=0) \ll 10^6 \text{ s}^{-1}$ .

To solve for  $\Gamma(\tau)$ , we take a Laplace transform for (73) with  $\Gamma(\tau=0^-) = 0$ . Together with (38) for the Laplace transform of  $Q$ , we write  $\Gamma(s)$  in terms of the response function  $f$ ,

$$\Gamma(s) = \frac{1}{s + K\beta(1 + s Q(s))/\hat{\lambda}} = \frac{s + \beta^{-1}s^{1/2} + \beta^{-1}}{D_2(s^{1/2})} \equiv f, \quad (74)$$

with the characteristic equation

$$D_2(z) = z^4 + \beta^{-1}z^3 + (K(3\hat{\lambda})^{-1} + \beta^{-1})z^2 + K\hat{\lambda}^{-1}z + K\hat{\lambda}^{-1}. \quad (75)$$

To invert  $f$  in (74), we recast it into following form:

$$f(s) = \frac{A_1}{(s^{1/2} + \gamma_1)} + \frac{A_2}{(s^{1/2} + \gamma_2)} + \frac{A_3}{(s^{1/2} + \gamma_3)} + \frac{A_4}{(s^{1/2} + \gamma_4)}, \quad (76)$$

where  $\gamma_1, \gamma_2, \gamma_3$ , and  $\gamma_4$  are the roots of  $D_2(-z) = 0$  in (75), and the coefficients  $A_1, A_2, A_3$ , and  $A_4$  are found to be

$$\begin{aligned} A_1 &= \frac{\gamma_1^2(\gamma_2\gamma_3 + \gamma_2\gamma_4 + \gamma_3\gamma_4 - 1)}{(\gamma_1 - \gamma_2)(\gamma_1 - \gamma_3)(\gamma_1 - \gamma_4)}, \\ A_2 &= \frac{\gamma_2^2(\gamma_1\gamma_3 + \gamma_1\gamma_4 + \gamma_3\gamma_4 - 1)}{(\gamma_2 - \gamma_1)(\gamma_2 - \gamma_3)(\gamma_2 - \gamma_4)}, \\ A_3 &= \frac{\gamma_3^2(\gamma_1\gamma_2 + \gamma_1\gamma_4 + \gamma_2\gamma_4 - 1)}{(\gamma_3 - \gamma_1)(\gamma_3 - \gamma_2)(\gamma_3 - \gamma_4)}, \\ A_4 &= \frac{\gamma_4^2(\gamma_1\gamma_2 + \gamma_1\gamma_3 + \gamma_2\gamma_3 - 1)}{(\gamma_4 - \gamma_1)(\gamma_4 - \gamma_2)(\gamma_4 - \gamma_3)}. \end{aligned} \quad (77)$$

Having (76) inverted using (39),  $\Gamma(\tau)$  can be readily determined as

$$\Gamma(\tau) = \sum_{n=1}^4 A_n \left[ \frac{1}{\sqrt{\pi}\sqrt{\tau}} - \gamma_n \exp(\gamma_n^2 \tau) \text{erfc}(\gamma_n \sqrt{\tau}) \right]. \quad (78)$$

For the no-slip case, the solution can be obtained in a similar fashion, as given by (D21) in Appendix D 3.

Figure 7(a) plots the time evolutions of the angular velocity  $\Gamma$  under  $\rho_p = \rho$  for both slip and no-slip cases using (78) and (D21). This figure reveals that slip effects can influence the angular dynamics of a particle in both short-time and long-time regimes. At short times, slip tends to delay the onset of viscous relaxation—the larger

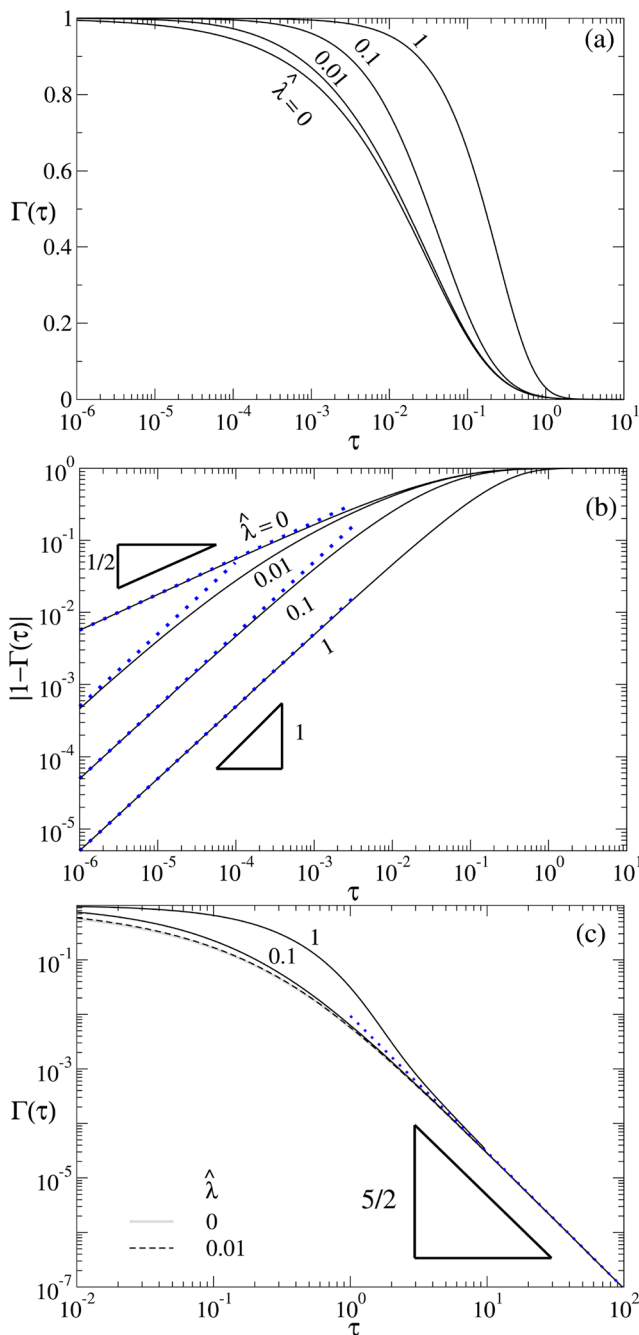


**FIG. 7.** (a) Temporal responses of the angular velocity  $\Gamma$  under  $\rho_p = \rho$  for slip and no-slip spheres when subjected to a torque impulse, described by (78) and (D21), respectively. Slip tends to delay the onset of viscous relaxation at short times but makes  $\Gamma$  decay faster afterward. (b) plots the corresponding short-time evolutions of the angular velocity relaxation  $\Gamma' = |1 - \Gamma|$ . Dotted lines represent the short-time asymptotes (80) found for the slip case and (D23) for the no-slip case, showing that the former varies as  $O(\tau)$ , very different from  $O(\tau^{1/2})$  for the latter. (c) plots the corresponding long-time responses, showing an  $O(\tau^{-5/2})$  attenuation irrespective of the slip length  $\hat{\lambda}$ . This is in accordance with the long-time asymptote (dotted line) given by (82).

the slip length  $\hat{\lambda}$ , the longer the time to initiate the decay from  $\Gamma = 1$ . However, after  $\Gamma$  starts off its decay, slip will make  $\Gamma$  decay faster afterward, and this trend will continue to the long-time regime.

Recall that the characteristic distinctions between the slip non-Basset kernel  $Q$  [see (40)] and the no-slip Basset kernel  $Q_B$  [see (44)] manifest mostly in the short-time regime [see Fig. 3(a)]. Figure 7(b) plots the short-time evolutions of the angular velocity relaxation  $\Gamma' = |1 - \Gamma|$  for both slip and no-slip cases calculated from (78) and (D23), respectively. The results clearly show that  $\Gamma'$  for the slip case behaves as  $O(\tau)$ , very different from  $O(\tau^{1/2})$  for the no-slip case. In addition, the larger the slip length  $\hat{\lambda}$ , the longer the time required for the  $O(\tau)$  response to begin its slowdown. Such dynamic distinctions also resemble those shown in Fig. 6 for the force impulse situation—they all are attributed to the characteristic differences between the slip non-Basset and the no-slip Basset kernels, as displayed in Figs. 2 and 3.

To explain the observed short-time responses for the slip case, we again carry out a large  $s$  expansion for (5.27),

$$\Gamma(s) = \frac{1}{s} - \frac{K}{3\hat{\lambda}} \frac{1}{s^2} + \frac{K}{3\hat{\lambda}^2} \frac{1}{s^{5/2}} + O(s^{-3}), \quad (79)$$

which leads to

$$\Gamma(\tau) = 1 - \frac{K}{3\hat{\lambda}} \tau + \frac{4K}{9\sqrt{\pi}\hat{\lambda}^2} \tau^{3/2} + O(\tau^{5/2}). \quad (80)$$

Equation (80) reveals the following features that are shown in Figs. 7(a) and 7(b). First, the first correction  $\Gamma^{(1)}$  due to viscous relaxation enters at  $O(\tau)$ . In the dimensional form,  $\Gamma$  attenuates linearly with time as  $-5(\mu/\rho_p\lambda a)t$ . Hence, not only will it take time  $t \sim \rho_p\lambda a/\mu$  proportional to the slip length  $\lambda$  to see a linear decay from the start-up constant angular velocity but also the amplitude of this linear attenuation will be increased as  $\lambda$  is decreased. Second, the second correction  $\Gamma^{(2)}$  goes as  $\sim (K/\hat{\lambda}^2)\tau^{3/2}$ . Because  $\Gamma^{(1)} \sim (K/\hat{\lambda})\tau$ , the transition from  $\Gamma^{(1)}$  to  $\Gamma^{(2)}$  will take place at  $\tau \sim \hat{\lambda}^2$  or  $t \sim \lambda^2/\nu$  corresponding to the slip-stick transition time. This explains why a slowdown of the  $O(\tau)$  response seen in Fig. 7(b) takes place at a longer time for larger  $\hat{\lambda}$ .

The  $O(\tau)$  attenuation at short times can be understood more physically by looking at a small  $\tau$  expansion of (73) for finding the angular velocity correction  $\Gamma^{(1)}$  to the leading contribution  $\Gamma^{(0)}$  due to a torque impulse,

$$\frac{d\Gamma^{(0)}}{d\tau} = \delta(\tau), \quad (81a)$$

$$\frac{d\Gamma^{(1)}}{d\tau} = -\frac{K}{1+3\hat{\lambda}} \left[ \Gamma^{(0)} + \int_0^\tau Q_{\ll}(\tau-\tau') \frac{d\Gamma^{(0)}}{d\tau'} d\tau' \right]. \quad (81b)$$

Here, the memory kernel  $Q_{\ll}$  in (81b) is taken as the short-time constant form due to (4.13):  $Q(\tau \rightarrow 0) = 1/3\hat{\lambda}$ . As can be clearly revealed from (81b),  $\Gamma^{(1)} = -(K/3\hat{\lambda})\tau$  is essentially a result of the memory torque  $(1+3\hat{\lambda})^{-1}K/3\hat{\lambda}$ , which dominates over the Stokes torque  $(1+3\hat{\lambda})^{-1}K$  when  $\hat{\lambda} \ll 1$ . It also suggests that for  $\rho_p = \rho$ , it will take time  $\tau \sim 3\hat{\lambda}/K \sim \hat{\lambda}/5$  to see an onset of viscous relaxation,



explaining why the larger  $\hat{\lambda}$  the longer time to start off the decay of  $\Gamma$  in the short-time regime shown in Fig. 7(a). For the no-slip case,  $\Gamma^{(1)} \sim O(\tau^{1/2})$  can be explained by using the same equations (81a) and (81b) with the Basset kernel (44) in the short-time form:  $Q_B(\tau \rightarrow 0) = 1/3(1/\sqrt{\pi\tau} - 1 + 2\sqrt{\tau}/\sqrt{\pi}) + O(\tau)$ .

Figure 7(c) plots the long-time response for both slip and no-slip cases calculated from (82) and (D24), respectively. The results clearly show that  $\Gamma$  decays as  $O(\tau^{-5/2})$ , irrespective of the amount of slip. To explain this, we determine the long-time  $\tau \gg 1$  response by taking a large  $\tau$  expansion for (78),

$$\Gamma(\tau) = \sum_{n=1}^4 A_n \left[ \frac{1}{\gamma_n^2 \sqrt{\pi}} \left(\frac{1}{\tau}\right)^{3/2} - \frac{3}{4\gamma_n^4 \sqrt{\pi}} \left(\frac{1}{\tau}\right)^{5/2} \right] + O(\tau^{-7/2}). \quad (82)$$

It can be shown that the  $O(\tau^{-3/2})$  term is identically zero, so the first contribution appears at  $O(\tau^{-5/2})$ . It can also be shown that the  $O(\tau^{-5/2})$  term is independent of the slip length  $\hat{\lambda}$ , in accordance with the result found by Ref. 56. As in the following, the coefficients of these terms can be evaluated analytically by taking derivatives with respect to  $z = s^{1/2}$  for the response function  $f$  given by (76):

$$\sum_{n=1}^4 \frac{A_n}{\gamma_n^2} = f'(0) = 0, \quad (83a)$$

$$\sum_{n=1}^4 \frac{A_n}{\gamma_n^4} = \frac{-1}{6} f'''(0) = \frac{-1}{3K}. \quad (83b)$$

The long-time response for the no-slip case can also be obtained in a similar manner. It has exactly the same  $O(\tau^{-5/2})$  attenuation as (82) because of (83), as shown in (D24) and (D3) in Appendix D 3.

#### D. Asynchronous particle spinning in an oscillatory vortical flow

A particle in a non-uniform flow often exhibits spinning due to the transverse flow gradient. In the last case study, we would like to explore the impacts of the additional slip-induced Faxen torque brought by an unsteady imposed flow. This can be revealed by examining the rotational response of a slip particle when it is subject to an oscillatory vortical flow:  $\mathbf{u}^\infty(\mathbf{x})e^{-i\omega t} = \mathbf{\Omega}^\infty \times \mathbf{x}e^{-i\omega t}$ . Restricting the particle Reynolds number  $Re_p = \Omega^\infty a^2/\nu$  to be small and letting  $\Gamma = \mathbf{\Omega}/\mathbf{\Omega}^\infty$  by rescaling the particle's angular velocity  $\mathbf{\Omega}$  with respect to  $\mathbf{\Omega}^\infty$  evaluated at the particle center, the angular Eq. (47) for the particle in the frequency domain with the torque expression (37) takes the following dimensionless form:

$$\alpha^2 \tilde{I}_p \Gamma = \alpha^2 \tilde{I}_f - (1 + 3\hat{\lambda})^{-1} \left( \frac{1 + \alpha + \alpha^2/3}{1 + \alpha + \beta\alpha^2} \right) \left[ \Gamma - 1 + \frac{\hat{\lambda}}{5} \alpha^2 \right], \quad (84)$$

where  $\tilde{I}_p = \tilde{I}_f(\rho_p/\rho)$  and  $\tilde{I}_f = 1/15$  represent the dimensionless rotational inertias for the particle and the fluid, respectively. With (84),  $\Gamma$  is therefore determined as

$$\Gamma = \frac{(1 + 3\hat{\lambda})\alpha^2 \tilde{I}_f + \left( \frac{1 + \alpha + \alpha^2/3}{1 + \alpha + \beta\alpha^2} \right) \left[ 1 - \frac{\hat{\lambda}}{5} \alpha^2 \right]}{(1 + 3\hat{\lambda})\alpha^2 \tilde{I}_p + \left( \frac{1 + \alpha + \alpha^2/3}{1 + \alpha + \beta\alpha^2} \right)}. \quad (85)$$

If there is no slip, a particle having  $\tilde{I}_p = \tilde{I}_f$  always rotates at  $\Gamma = 1$  regardless of the value of  $\alpha$ . This is because in this case, the fluid's rotational momentum is fully transferred to the particle, making the particle spin like a rigid body along with the fluid. Either  $\hat{\lambda} \neq 0$  or  $\tilde{I}_p \neq \tilde{I}_f$  will make a particle spin at an unequal rate. To gain more insight into how the particle spinning responds, we inspect both low frequency and high frequency situations below.

At low frequencies  $|\alpha| \ll 1$ , (85) becomes

$$\Gamma = 1 + \left[ -(1 + 3\hat{\lambda}) \left( \frac{\rho_p}{\rho} - 1 \right) \tilde{I}_f - \frac{\hat{\lambda}}{5} \right] \alpha^2 + O(\alpha^3). \quad (86)$$

In the steady limit  $|\alpha| \rightarrow 0$ , the particle again rotates with the flow at  $\Gamma = 1$  because of the precise transmission of the Stokes torque from the fluid to the particle. When the flow is oscillating at a small frequency, the particle's rotational velocity correction  $\Gamma' = (\mathbf{\Omega} - \mathbf{\Omega}^\infty)/\mathbf{\Omega}^\infty = \Gamma - 1$  is found at  $O(\alpha^2)$ , as indicated by (86). This  $O(\alpha^2)$  correction can be interpreted as a result by balancing the instantaneous Stokes torque to the fluid's and the particle's inertial rotations at  $O(\alpha^2)$  in (84),

$$\alpha^2 \tilde{I}_p \Gamma' = \alpha^2 \tilde{I}_f - (1 + 3\hat{\lambda})^{-1} \left[ \Gamma' + \frac{\hat{\lambda}}{5} \alpha^2 \right]. \quad (87)$$

In the case of no slip  $\hat{\lambda} = 0$ ,  $\Gamma'$  will be determined purely by the mismatch in rotational inertia between the particle's  $\tilde{I}_p$  and the fluid's  $\tilde{I}_f$ . This will make the particle spinning slow down if  $\rho_p > \rho$  or speed up otherwise. If it happens to  $\tilde{I}_p = \tilde{I}_f$  when  $\rho = \rho_p$ ,  $\Gamma'$  will occur at  $O(\alpha^3)$  when  $\hat{\lambda} = 0$ . Interestingly, if there is slip under this equal rotational inertia situation, not only will  $\Gamma'$  be changed back to  $O(\alpha^2)$  but also the particle spinning will be slowed down by slip through the  $\hat{\lambda}\alpha^2$  term.

At high frequencies  $|\alpha| \gg 1$ , (85) behaves as

$$\Gamma = \frac{\tilde{I}_f}{\tilde{I}_p \hat{\lambda}} \left( \frac{1}{\alpha} \right) + O(\alpha^{-2}). \quad (88)$$

In this regime, both the fluid's and the particle's inertia torques in (84) dominate at  $O(\alpha^2)$ . A closer inspection of (84) reveals that when  $|\alpha|$  is large, the fluid's inertial torque  $\alpha^2 \tilde{I}_f$  is nearly canceled out by the slip-induced torque  $(1 + 3\hat{\lambda})^{-1} \hat{\lambda} \alpha^2/5$ , making  $\Gamma \rightarrow 0$  as  $|\alpha| \rightarrow \infty$ . Note that such zero spinning as  $|\alpha| \rightarrow \infty$  is absent in the no-slip case whose  $\Gamma \rightarrow \tilde{I}_f/\tilde{I}_p$  is finite as  $|\alpha| \rightarrow \infty$ . (88) indicates that  $\Gamma$  at large  $|\alpha|$  behaves as  $\Gamma_{\gg} = (\tilde{I}_f/\tilde{I}_p) \hat{\lambda}^{-1} \alpha^{-1}$  due to viscous torque. Increasing slip reduces  $\Gamma_{\gg}$  because of less viscous shearing on the particle. In the bubble limit as  $\hat{\lambda} \rightarrow \infty$ ,  $\Gamma_{\gg} \rightarrow 0$  because the particle will not feel viscous shearing from the fluid at all. In fact, such zero spinning response as  $\hat{\lambda} \rightarrow \infty$  is not limited to large  $|\alpha|$  but actually happens to an arbitrary value of  $|\alpha|$ , as can be seen from (84).

Having gleaned the features for both  $|\alpha| \ll 1$  and  $|\alpha| \gg 1$  shown above, we now inspect how  $|\Gamma|$  varies with  $|\alpha|$  in more detail. As shown in Fig. 8(a), for  $\rho_p > \rho$ , the particle spins slower than the flow and its spinning is always slowed down by increasing  $|\alpha|$ . For a given value of  $|\alpha|$ , slip always diminishes the particle rotation. The responses for  $\rho_p = \rho$  are also similar to those for  $\rho_p > \rho$ , as shown in Fig. 8(b). Recall in this case that a no-slip particle

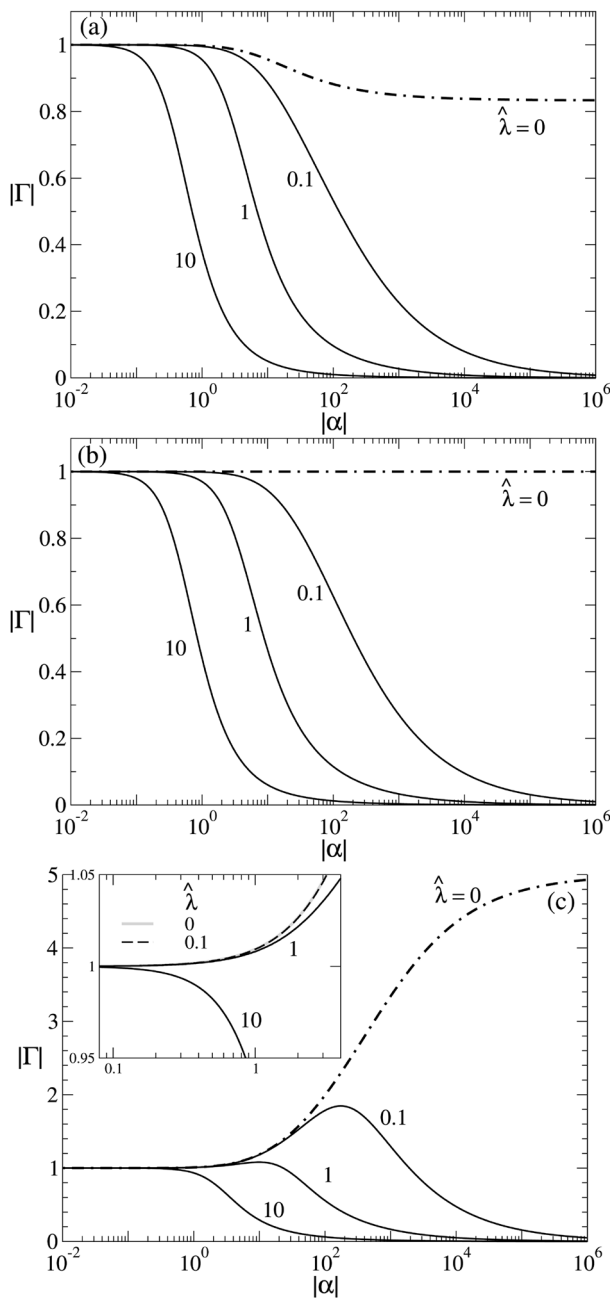


**FIG. 8.** Behavior of the angular velocity amplitude  $|\Gamma| = |\Omega|/|\Omega_\infty|$  described by (85) for the spinning of a slip particle in an oscillatory vortical flow. Plots show how  $|\Gamma|$  varies with the dimensionless frequency  $|\alpha| = (\omega a^2/\nu)^{1/2}$  and the slip length  $\hat{\lambda}$ . (a) illustrates the heavy particle  $\rho_p > \rho$  case with  $l_p = 1.2 \times l_f$ , showing that the particle spins slower than the flow with  $|\Gamma| < 1$  and that  $|\Gamma|$  decreases monotonically with  $|\alpha|$ . (b) plots the equal density  $\rho_p = \rho$  case, showing similar responses to (a). Note that a no-slip particle in this special situation has  $\Gamma = 1$  irrespective of the value of  $|\alpha|$ . (c) illustrates the light particle  $\rho_p < \rho$  case with  $l_p = 0.2 \times l_f$ . In this case, the particle can spin faster than the flow at small  $|\alpha|$  and become slower at large  $|\alpha|$ . In all cases,  $|\Gamma|$  with slip is always smaller than that without slip and increasing  $\hat{\lambda}$  lowers  $|\Gamma|$ . Also note that in the  $|\alpha| \rightarrow \infty$  limit, the slip case reduces to the bubble case with  $|\Gamma| = 0$  in contrast to  $|\Gamma| \neq 0$  for the no-slip case.

always spins at the same rate as the flow. For  $\rho_p < \rho$ , on the contrary, the results are very different. As shown in Figs. 8(c) and 8(a), the particle can spin faster or slower than the flow, depending on  $|\alpha|$ . For small  $|\alpha|$ ,  $|\Gamma| > 1$  and increases with  $|\alpha|$ .  $|\Gamma|$  then reaches a peak at some value of  $|\alpha|$  after which it declines with  $|\alpha|$ . Further increasing  $|\alpha|$  will eventually make  $|\Gamma| < 1$ . Note that such a non-monotonic spinning response exists only when slip is present. In any case, if slip effects are sufficiently strong, a particle will hardly rotate because of the lack of the viscous shearing by the surrounding fluid.

## VI. CONCLUSIONS AND PERSPECTIVES

We have demonstrated the non-Basset particle dynamics arising from slip effects. We find that even a tiny amount of slip can cause dramatic impacts on particle motion. Impacts of slip are mainly reflected by the atypical non-Basset memory kernels when the slip length is small. This makes a slip particle in unsteady motion behave very different from a no-slip particle, as well as from a fluid particle.

Compared to a no-slip particle and a full slip bubble, the dynamic distinctions of a slip particle, in particular, manifest in the short time or high frequency regime. In transient particle sedimentation, the short-time correction to constant acceleration for a slip particle is found to occur at  $O(t^2)$ , in contrast to  $O(t^{3/2})$  for a no-slip particle. A similar result can also be found in the translational response of a slip particle to a suddenly applied stream, showing an  $O(t)$  viscous relaxation instead of  $O(t^{1/2})$  for a no-slip particle. In these transient translational problems, while a full slip bubble basically behaves like a partial slip particle in their velocity responses at very short times, their later time responses differ qualitatively, distinguished by the existence of the inherent slip-stick transition for a partial slip particle but not for a bubble. This highlights the fact that even though both slip and bubble cases have the same type of non-Basset memory kernels, they do not necessarily imply the same physics. For transient rotation, the same dynamic change from  $O(t^{1/2})$  for a no-slip particle to  $O(t)$  for a slip particle can also be observed in the angular response of the latter to a torque impulse. However, for a bubble, it will not undergo any rotation at all because of the lack of viscous shearing on its surface. This is another characteristic distinction between a partial slip particle and a full slip bubble.

Perhaps the most pronounced effects can be realized by having a slip particle undergo periodic spinning in an oscillatory vortical flow. We find that slip can introduce an additional inertia torque to slow down the particle spinning in the high frequency regime. It is also this torque responsible for the non-monotonic spinning response of a slip particle when it is lighter than the surrounding fluid. We emphasize that without this torque, it is not possible to guarantee that a strongly slip particle will not rotate at all in the bubble limit.

As these non-Basset motion responses of slip particles are very sensitive to the amount of slip, they may serve as alternative means to quantify the extent of fluid slippage on colloidal particles such as those made by polymers or with hydrophobic coating. They may also have potential in realizing more efficient hydrodynamic sorting of slip particles from no-slip or fluid particles.

From a dynamical perspective, it has been shown that no-slip particles are less inclined to accumulate locally or tend to diminish the formation of attractors,<sup>57,58</sup> largely due to the memory effects brought by the Basset history force that is singular at  $t = 0$  and always varies as  $t^{-1/2}$  in the time scale of the typical viscous relaxation time  $t_\nu = a^2/\nu$ . For slip particles, in contrast, the history force is of non-Basset type. Such a force behaves very differently than the Basset force in that it will not only start with a finite value at  $t = 0$  but also vary non-uniformly with time, depending not only on  $t_\nu$  but also on the slip-stick transition time  $t_\lambda = \lambda^2/\nu$ . Together with the fact that the finite size effects and additional inertial torque from an imposed flow could make a slip particle deviated and dis-aligned from the flow, it is likely that a slip particle in the presence of flows may display completely different dynamics than a no-slip particle. Along this line, many other aspects such as particle mixing/dispersion, inertial trapping, and routes to chaos will likely be altered by slip effects as opposed to those described by the classical Maxey–Riley equation. These dynamical aspects will demand more in-depth investigations, and the present work will provide the framework for such tasks.

The present work will also provide a consistent formalism capable of describing a variety of particle-laden flows. This is particularly appealing to those involving aerosols or hydrophobic particles to which the Maxey–Riley equation may no longer be applicable due to considerable fluid slippage on the surfaces of such particles. Overall, we have demonstrated that effects of slip can strongly influence the fate of a particle in unsteady motion. This may change the current understanding of inertial particle dynamics as occurring to aerosol suspensions, turbulent particle flows, and unsteady swimming of self-propelled microorganisms.

### ACKNOWLEDGMENTS

This work was supported by the Ministry of Science and Technology of Taiwan under the Grant No. MOST 108-2811-E-006-511.

### APPENDIX A: DERIVATION OF $\mathcal{R}^T$ (20)

Following Ref. 52, the flow field produced by an oscillating sphere can be expressed as a linear combination of oscillatory Stokeslet  $\mathbf{S}$  and dipole  $\mathbf{D}$ ,

$$\hat{\mathbf{u}} = \left[ \frac{g}{8\pi} \mathbf{S} + \frac{d}{4\pi} \mathbf{D} \right] \cdot \mathbf{U}, \quad (\text{A1})$$

with  $g$  and  $d$  being the corresponding strengths. Let  $\tilde{r} = \alpha r/a$ . The Stokeslet  $\mathbf{S}$  is given by

$$\mathbf{S} = A(\tilde{r})(\mathbf{I}/r) + B(\tilde{r})(\mathbf{x} \mathbf{x}/r^3), \quad (\text{A2})$$

with

$$A = 2e^{-\tilde{r}} \left( 1 + \frac{1}{\tilde{r}} + \frac{1}{\tilde{r}^2} \right) - \frac{2}{\tilde{r}^2}, \quad B = -2e^{-\tilde{r}} \left( 1 + \frac{3}{\tilde{r}} + \frac{3}{\tilde{r}^2} \right) + \frac{6}{\tilde{r}^2}.$$

The dipole  $\mathbf{D}$  is

$$\mathbf{D} = -C(\tilde{r})(\mathbf{I}/r^3) + 3H(\tilde{r})(\mathbf{x} \mathbf{x}/r^5), \quad (\text{A3})$$

with

$$C = e^{-\tilde{r}}(1 + \tilde{r} + \tilde{r}^2), \quad H = e^{-\tilde{r}} \left( 1 + \tilde{r} + \frac{\tilde{r}^2}{3} \right).$$

The coefficients  $g$  and  $d$  in (A1) can be determined using boundary conditions on the sphere surface at  $r = a$ ,  $(\hat{\mathbf{u}} - \mathbf{U}) \cdot (\mathbf{I} - \mathbf{nn}) = \lambda [\nabla \hat{\mathbf{u}} + (\nabla \hat{\mathbf{u}})^T] \cdot \mathbf{n} \cdot (\mathbf{I} - \mathbf{nn})$  and  $(\hat{\mathbf{u}} - \mathbf{U}) \cdot \mathbf{n} = 0$ ,

$$g = \frac{3a}{4} \left[ \left( \frac{1 + 2\hat{\lambda}}{1 + 3\hat{\lambda}} \right) \left( \frac{\alpha + 1}{1 + \beta\alpha} \right) + \frac{\alpha^2}{3} \right], \quad (\text{A4})$$

$$d = \frac{a^3}{2} \left[ 1 + \frac{3(\alpha + 1 - e^\alpha)(1 + 2\hat{\lambda})}{\alpha^2((\alpha + 3)\hat{\lambda} + 1)} \right], \quad (\text{A5})$$

where  $\hat{\lambda} = \lambda/a$  is the dimensionless slip length.

The stress associated with Stokeslet (A2) takes the form of

$$\mathbf{t}_S = \mu g \left[ \frac{\mathbf{I}}{r^2} K(\tilde{r}) + \frac{\mathbf{x} \mathbf{x}}{r^4} L(\tilde{r}) \right] \cdot \mathbf{U}, \quad (\text{A6})$$

with  $K(\tilde{r}) = 2[B(\tilde{r}) - e^{-\tilde{r}}(\tilde{r} + 1)]$  and  $L(\tilde{r}) = 2[e^{-\tilde{r}}(\tilde{r} + 1) - 1 - 3B(\tilde{r})]$ . Evaluating (A6) at  $r = a$  together with (A4) gives the surface stress on the sphere,

$$\mathbf{t}_S = \frac{-3\mu\mathbf{U}}{2a} \left[ \frac{(\alpha + 1)}{(\alpha + 3)\hat{\lambda} + 1} \right] \cdot \mathbf{I}. \quad (\text{A7})$$

The part associated with dipole (A3) is

$$\mathbf{t}_D = \mu d \left[ \frac{\mathbf{I}}{r^4} M(\tilde{r}) + \frac{\mathbf{x} \mathbf{x}}{r^4} N(\tilde{r}) \right] \cdot \mathbf{U}, \quad (\text{A8})$$

with  $M(\tilde{r}) = e^{-\tilde{r}}(6 + 6\tilde{r} + 3\tilde{r}^2 + \tilde{r}^3)$  and  $N(\tilde{r}) = -e^{-\tilde{r}}(18 + 18\tilde{r} + 7\tilde{r}^2 + \tilde{r}^3)$ . The corresponding surface stress on the sphere can be determined using (A8) at  $r = a$  and (A5),

$$\mathbf{t}_D = \frac{-\mu\mathbf{U}}{2a} \left[ \frac{18(\tilde{r} + 1)\hat{\lambda}}{(\tilde{r} + 3)\hat{\lambda} + 1} + \tilde{r}^2 \right] \cdot \mathbf{nn}. \quad (\text{A9})$$

Adding (A7) and (A9) yields the translation resistance density matrix  $\mathcal{R}^T$  given by (20).

### APPENDIX B: DERIVATION OF $\mathcal{R}^R$ (33)

As in Ref. 52, the flow field around a sphere undergoing rotary oscillations can be thought of as the fluid motion set up by an oscillatory rotlet,

$$\hat{\mathbf{u}} = \frac{b}{8\pi\mu} \boldsymbol{\Omega} \times \frac{\mathbf{x}}{r^3} e^{-\tilde{r}}(1 + \tilde{r}). \quad (\text{B1})$$

The strength  $b$  can be determined using the slip boundary condition  $(\hat{\mathbf{u}} - \boldsymbol{\Omega} \times \mathbf{x}) \cdot (\mathbf{I} - \mathbf{nn}) = \lambda [\nabla \hat{\mathbf{u}} + (\nabla \hat{\mathbf{u}})^T] \cdot \mathbf{n} \cdot (\mathbf{I} - \mathbf{nn})$  at  $r = a$ ,

$$b = \frac{8\pi\mu a^3 e^\alpha}{(1 + \alpha)(1 + 3\hat{\lambda}) + \hat{\lambda}\alpha^2}. \quad (\text{B2})$$

With  $\hat{\sigma}^R = \mu(\nabla\hat{\mathbf{u}} + (\nabla\hat{\mathbf{u}})^T)$  because of pressure  $\hat{p} = 0$ , the surface stress corresponding to (B1) can be evaluated as

$$\hat{\sigma}^R \cdot \mathbf{n} = \frac{-b}{8\pi a^4} (\boldsymbol{\Omega} \times \mathbf{x}) (3(1 + \alpha) + \alpha^2) e^{-\alpha}. \quad (\text{B3})$$

With (B2), (B3) leads to the rotation resistance density matrix  $\mathcal{R}^R$  given by (33).

### APPENDIX C: DERIVATION OF THE ADDITIONAL UNSTEADY FAXEN TORQUE (35) BROUGHT BY SLIP

The purpose of this appendix is to evaluate the following integral that leads to (35):

$$\int_{S_p} \mathbf{x} \times \left[ \frac{\lambda}{\mu} (\mathbf{I} - \mathbf{nn}) \cdot (\boldsymbol{\sigma}^\infty \cdot \mathbf{n}) \cdot \mathcal{R}^R \right] dS. \quad (\text{C1})$$

With (33), (C1) can be evaluated as

$$\mathcal{I}_p = -3\hat{\lambda} \left[ \frac{1 + \alpha + \alpha^2/3}{(1 + \alpha)(1 + 3\hat{\lambda}) + \hat{\lambda}\alpha^2} \right] (T_{1p} - T_{2p}), \quad (\text{C2})$$

which consists of two contributions,

$$T_{1p} = \int_{S_p} \varepsilon_{j pq} x_q (\sigma_{jm}^\infty \cdot \mathbf{n}_m) dS, \quad (\text{C3})$$

$$T_{2p} = \int_{S_p} \varepsilon_{j pq} x_q n_j n_k (\sigma_{km}^\infty \cdot \mathbf{n}_m) dS. \quad (\text{C4})$$

The evaluation of (C3) can be done after substitution of (22) together with  $I_{qm} = \int_{S_p} n_q n_m dS = (4/3)\pi a^2 \delta_{qm}$  and  $I_{qmst} = \int_{S_p} n_q n_m n_s n_t dS = (4/15)\pi a^2 (\delta_{qm} \delta_{st} + \delta_{qs} \delta_{mt} + \delta_{qt} \delta_{ms})$ ,

$$\begin{aligned} T_{1p} &= a \int_{S_p} \varepsilon_{j pq} n_q n_m \sigma_{jm}^\infty(0) dS + \frac{a^3}{2} \int_{S_p} \varepsilon_{j pq} n_q n_m n_t \left. \frac{\partial^2 \sigma_{jm}^\infty}{\partial x_l \partial x_l} \right|_0 dS \\ &= \frac{4}{3} \pi a^3 \varepsilon_{j pq} \sigma_{jq}^\infty(0) + \frac{4}{30} \pi a^5 (\varepsilon_{j pm} \delta_{lt} + \varepsilon_{j pl} \delta_{mt} + \varepsilon_{j pl} \delta_{ml}) \left. \frac{\partial^2 \sigma_{jm}^\infty}{\partial x_l \partial x_l} \right|_0 \\ &= \frac{4}{15} \pi a^5 \varepsilon_{j pl} \left. \frac{\partial^2 \sigma_{jm}^\infty}{\partial x_m \partial x_l} \right|_0 \\ &= \frac{4}{15} \pi a^5 \nabla \times (\nabla \cdot \boldsymbol{\sigma}^\infty). \end{aligned} \quad (\text{C5})$$

The  $\sigma_{jm}^\infty(0)$  term vanishes because  $\varepsilon_{j pq} \sigma_{jq}^\infty = 0$ . Similarly, (C4) can be evaluated as

$$\begin{aligned} T_{2p} &= a \int_{S_p} \varepsilon_{j pq} n_q n_j n_k n_m \sigma_{km}^\infty(0) dS \\ &\quad + \frac{a^3}{2} \int_{S_p} \varepsilon_{j pq} n_q n_j n_k n_m n_t \left. \frac{\partial^2 \sigma_{jm}^\infty}{\partial x_m \partial x_l} \right|_0 dS \\ &= \frac{4}{15} \pi a^3 \varepsilon_{j pq} (\delta_{qj} \delta_{km} + \delta_{qk} \delta_{jm} + \delta_{qm} \delta_{kj}) \sigma_{km}^\infty(0) \\ &\quad + \frac{a^3}{2} \varepsilon_{j pq} \left. \frac{\partial^2 \sigma_{jm}^\infty}{\partial x_m \partial x_l} \right|_0 \int_{S_p} n_q n_j n_k n_m n_t dS. \end{aligned} \quad (\text{C6})$$

The  $\sigma_{km}^\infty(0)$  term is zero because it involves  $\varepsilon_{j pq} I_{qjkm}$ . The  $\nabla \times \nabla \cdot \sigma_{jm}^\infty|_0$  term involves the integration of the sixth order isotropic tensor,

$$\begin{aligned} \int_{S_p} n_q n_j n_k n_m n_l n_t dS &= \frac{4\pi a^2}{105} [\delta_{km} A_{qjlt} + \delta_{kj} A_{qmlt} \\ &\quad + \delta_{kq} A_{jmlt} + \delta_{kl} A_{qjmt} + \delta_{kt} A_{qjml}], \end{aligned} \quad (\text{C7})$$

where  $A_{ijkl} = \delta_{ij} \delta_{kl} + \delta_{ik} \delta_{jl} + \delta_{il} \delta_{jk}$ . Using (C7), we find that the  $\nabla \times \nabla \cdot \sigma_{jm}^\infty|_0$  term is identically zero. Combining (C5) and (C6) gives (35).

### APPENDIX D: TRANSIENT RESPONSES OF NO-SLIP SPHERES

To compare our new results due to slip in Secs. V A–V C, we also analyze the corresponding motions of no-slip spheres by solving the equations of motion (31) and (43) with  $\hat{\lambda} = 0$ .

#### 1. Transient sedimentation

The dimensionless equation of the particle motion (49) is reduced to

$$M \frac{dV}{d\tau} = 1 - V - \int_0^\tau G_B(\tau - \tau') \frac{dV}{d\tau'} d\tau', \quad (\text{D1})$$

with  $G_B(\tau) = 1/\sqrt{\pi\tau}$  being the Basset kernel. Taking a Laplace transform for (D1) gives

$$\begin{aligned} V(s) &= \frac{1}{Ms} \left[ \frac{1}{s + M^{-1}s^{1/2} + M^{-1}} \right] \\ &= \frac{1}{Ms} \frac{1}{\gamma_2 - \gamma_1} \left( \frac{1}{s^{1/2} + \gamma_1} - \frac{1}{s^{1/2} + \gamma_2} \right), \end{aligned} \quad (\text{D2})$$

where

$$\gamma_1 = \frac{1 + \sqrt{1 - 4M}}{2M}, \quad \gamma_2 = \frac{1 - \sqrt{1 - 4M}}{2M}. \quad (\text{D3})$$

An analytical solution for  $V(\tau)$  can be obtained after taking an inversion using (53),

$$\begin{aligned} V(\tau) &= 1 + \frac{1}{M(\gamma_2 - \gamma_1)} \left[ -\frac{1}{\gamma_1} \exp(\gamma_1^2 \tau) \operatorname{erfc}(\gamma_1 \sqrt{\tau}) \right. \\ &\quad \left. + \frac{1}{\gamma_2} \exp(\gamma_2^2 \tau) \operatorname{erfc}(\gamma_2 \sqrt{\tau}) \right]. \end{aligned} \quad (\text{D4})$$

At short times  $\tau \ll 1$ , (D4) has the following asymptotic behavior:

$$V(\tau) = \frac{\tau}{M} - \frac{4}{3\sqrt{\pi}} \frac{\tau^{3/2}}{M^2} + O(\tau^2), \quad (\text{D5})$$

which can also be obtained by inverting the large  $s$  expansion of (D2),

$$V(s) = \frac{1}{M} \left[ \frac{1}{s^2} - \frac{1}{Ms^{5/2}} \right] + O(s^{-3}).$$

The leading contribution is constant acceleration  $V^{(0)}(\tau) = \tau/M$ , giving the velocity  $U_M(t) = tF_g/(m_p + m_f/2)$  in the dimensional form. The viscous correction is found to occur at  $O(\tau^{3/2})$ . This  $O(\tau^{3/2})$  correction can be interpreted as the velocity acceleration by the Basset force  $F_B(t) \sim \sigma_B(t)a^2 \propto t^{1/2}$  setup by the shear stress  $\sigma_B(t) \sim \mu U_M(t)/\delta(t)$  across the viscous boundary layer of thickness  $\delta(t) \sim (vt)^{1/2}$ . This can be seen more clearly from the following equation for finding the correction velocity  $V^{(1)}$ :

$$M \frac{dV^{(1)}}{d\tau} = - \frac{dV^{(0)}}{d\tau} \int_0^\tau G_B(\tau - \tau') d\tau'. \quad (D6)$$

Note that in (D6), the Stokes drag  $-V^{(0)}(\tau)$  contributes to  $O(\tau)$  and thus is of a higher order contribution.

As for long times  $\tau \gg 1$ , (D4) behaves as

$$V(\tau) = 1 - \frac{1}{\sqrt{\pi}\sqrt{\tau}} + \dots, \quad (D7)$$

which can also be inferred from the small  $s$  expansion of (D2):  $V(s) = 1/s - 1/\sqrt{s} + \dots$ .

## 2. Translational response to a suddenly applied stream

The dimensionless Eq. (63) with  $\hat{\lambda} = 0$  is reduced to

$$M \frac{dV}{d\tau} = M(V_{start} - V_i) \frac{dH}{d\tau} + J \frac{dH}{d\tau} - V - \int_0^\tau G_B(\tau - \tau') \frac{dV}{d\tau'} d\tau' - G_B(\tau)V_i + [H(\tau) + G_B(\tau)] \left[ 1 + \frac{k}{6} \right]. \quad (D8)$$

The Laplace transform of (D8) with  $V(\tau = 0^-) = V_i$  is

$$V(s) = \frac{J'}{Ms} \left[ 1 + \frac{a_1 s^{1/2} + a_0}{s + M^{-1} s^{1/2} + M^{-1}} \right], \quad (D9)$$

where  $J' = MV_{start} + J$ ,  $a_0 = (1 + k/6)J' - M^{-1}$ , and  $a_1 = a_0 - V_i J'$ . We recast (D9) in the following form:

$$V(s) = \frac{J'}{Ms} \left[ 1 + \frac{B_1}{s^{1/2} + \gamma_1} + \frac{B_2}{s^{1/2} + \gamma_2} \right], \quad (D10)$$

where  $\gamma_1$  and  $\gamma_2$  are given in (D3) and

$$B_1 = \frac{\gamma_1 a_1 - a_0}{\gamma_1 - \gamma_2}, \quad B_2 = \frac{\gamma_2 a_1 - a_0}{\gamma_2 - \gamma_1}.$$

Using (53), we can invert (D10) as

$$V(\tau) = \frac{J'}{M} \left\{ 1 + \sum_{n=1}^2 B_n \gamma_n^{-1} \left[ 1 - \exp(\gamma_n^2 \tau) \operatorname{erfc}(\gamma_n \sqrt{\tau}) \right] \right\}. \quad (D11)$$

For short times  $\tau \ll 1$ , taking large  $s$  expansion for (D9) gives

$$V(s) = \frac{J'}{Ms} \left( 1 + s^{-1/2} a_1 \right) + O(s^{-2}), \quad (D12)$$

and hence, its inversion

$$V(\tau) = \frac{J'}{M} \left[ 1 + \frac{2a_1}{\sqrt{\pi}} \sqrt{\tau} \right] + O(\tau). \quad (D13)$$

For long times  $\tau \gg 1$ , (D9) in a small  $s$  expansion is

$$V(s) = \frac{1}{s} \left( 1 + \frac{k}{6} \right) + \left( \frac{a_1}{a_0} - 1 \right) \frac{J'}{s^{1/2}} + \dots, \quad (D14)$$

which leads to

$$V(\tau) = \left( 1 + \frac{k}{6} \right) + \left( \frac{a_1}{a_0} - 1 \right) \frac{J'}{\sqrt{\pi\tau}} + \dots. \quad (D15)$$

## 3. Angular response to a torque impulse

For  $\hat{\lambda} = 0$ , the angular dynamics are governed by the following dimensionless equation reduced from (73):

$$\frac{d\Gamma}{d\tau} = \delta(\tau) - K\Gamma - K \int_0^\tau Q_B \frac{d\Gamma}{d\tau'} d\tau', \quad (D16)$$

with the rotational Basset memory kernel  $Q_B$  given by (44) and  $K = 8\pi\rho a^5/I_p = 15\rho/\rho_p$ . The Laplace transform of (D16) with  $\Gamma(\tau = 0^-) = 0$  is

$$\Gamma(s) = \frac{s^{1/2} + 1}{D_3(s^{1/2})} \equiv h, \quad (D17)$$

with the characteristic equation

$$D_3(z) = z^3 + \left( 1 + \frac{K}{3} \right) z^2 + Kz + K. \quad (D18)$$

The response function  $h$  given by (D17) can be rewritten in the following form:

$$h(s) = \frac{A_1}{s^{1/2} + \gamma_1} + \frac{A_2}{s^{1/2} + \gamma_2} + \frac{A_3}{s^{1/2} + \gamma_3}, \quad (D19)$$

where  $\gamma_1, \gamma_2$ , and  $\gamma_3$  are the roots of  $D_3(-z) = 0$  in (D18) with the coefficients  $A_1, A_2$ , and  $A_3$  given by

$$A_1 = \frac{1 - \gamma_1}{(\gamma_1 - \gamma_2)(\gamma_1 - \gamma_3)}, \quad A_2 = \frac{1 - \gamma_2}{(\gamma_2 - \gamma_1)(\gamma_2 - \gamma_3)},$$

$$A_3 = \frac{1 - \gamma_3}{(\gamma_3 - \gamma_1)(\gamma_3 - \gamma_2)}. \quad (D20)$$

$\Gamma(\tau)$  can be obtained by inverting (D19) using (39), yielding

$$\Gamma(\tau) = \sum_{n=1}^3 A_n \left[ \frac{1}{\sqrt{\pi}\sqrt{\tau}} - \gamma_n \exp(\gamma_n^2 \tau) \operatorname{erfc}(\gamma_n \sqrt{\tau}) \right]. \quad (D21)$$

For short times  $\tau \ll 1$ , taking a large  $s$  expansion for (D17) gives

$$\Gamma(s) = \frac{1}{s} - \frac{K}{3} \frac{1}{s^{3/2}} + O(s^{-2}), \quad (D22)$$

and hence,

$$\Gamma(\tau) = 1 - \frac{2K}{3\sqrt{\pi}}\sqrt{\tau} + O(\tau). \quad (\text{D23})$$

The long-time  $\tau \gg 1$  behavior can be determined as follows by taking a large  $\tau$  expansion for (D21):

$$\Gamma(\tau) = \sum_{n=1}^3 A_n \left[ \frac{1}{\gamma_n^2 \sqrt{\pi}} \left(\frac{1}{\tau}\right)^{3/2} - \frac{3}{4\gamma_n^4 \sqrt{\pi}} \left(\frac{1}{\tau}\right)^{5/2} \right] + O(\tau^{-7/2}). \quad (\text{D24})$$

Using (D17) and (D19), both the  $O(\tau^{-3/2})$  and the  $O(\tau^{-5/2})$  terms can be readily evaluated according to

$$\sum_{n=1}^3 \frac{A_n}{\gamma_n^2} = h'(0) = 0, \quad (\text{D25a})$$

$$\sum_{n=1}^3 \frac{A_n}{\gamma_n^4} = \frac{-1}{6} h'''(0) = \frac{-1}{3K}. \quad (\text{D25b})$$

Here, the primes mean the derivatives with respect to  $z = s^{1/2}$ .

## DATA AVAILABILITY

The data that support the findings of this study are available within the article.

## REFERENCES

- <sup>1</sup>S. Wang and A. M. Ardekani, "Unsteady swimming of small organisms," *J. Fluid Mech.* **702**, 286–297 (2012).
- <sup>2</sup>I. Fouxon and Y. Or, "Inertial self-propulsion of spherical microswimmers by rotation-translation coupling," *Phys. Rev. Fluids* **4**, 023101 (2019).
- <sup>3</sup>S. Wang, J. S. Allen, and A. M. Ardekani, "Unsteady particle motion in an acoustic standing wave field," *Eur. J. Comput. Mech.* **26**, 115–130 (2017).
- <sup>4</sup>A. Krafcik, P. Babinec, M. Babincova, and I. Frollo, "Importance of Basset history force for the description of magnetically driven motion of magnetic particles in air," *Meas. Sci. Rev.* **20**, 50–58 (2020).
- <sup>5</sup>K. Guseva, A. Daitche, U. Feudel, and T. Tél, "History effects in the sedimentation of light aerosols in turbulence: The case of marine snow," *Phys. Rev. Fluids* **1**, 074203 (2016).
- <sup>6</sup>T. A. House, V. H. Lieu, and D. T. Schwartz, "A model for inertial particle trapping locations in hydrodynamic tweezers arrays," *J. Micromech. Microeng.* **24**, 045019 (2014).
- <sup>7</sup>S. Olivieri, F. Picano, G. Sardina, D. Iudicone, and L. Brandt, "The effect of the Basset history force on particle clustering in homogeneous and isotropic turbulence," *Phys. Fluids* **26**, 041704 (2014).
- <sup>8</sup>M. R. Maxey and J. J. Riley, "Equation of motion for a small rigid sphere in a nonuniform flow," *Phys. Fluids* **26**, 883–889 (1983).
- <sup>9</sup>M. R. Maxey, "The equation of motion for a small rigid sphere in a nonuniform or unsteady flow," *Trans. ASME J. Fluids Eng.* **116**, 57–62 (1993).
- <sup>10</sup>G. Haller, "Solving the inertial particle equation with memory," *J. Fluid Mech.* **874**, 1–4 (2019).
- <sup>11</sup>S. G. Prasath, V. Vasan, and R. Govindarajan, "Accurate solution method for the Maxey–Riley equation, and the effects of Basset history," *J. Fluid Mech.* **868**, 428–460 (2019).
- <sup>12</sup>S. Boi, "Exact results on the large-scale stochastic transport of inertial particles including the Basset history term," *Phys. Fluids* **31**, 063304 (2019).
- <sup>13</sup>A. B. Basset, "On the motion of a sphere in a viscous liquid," *Philos. Trans. R. Soc., A* **179**, 43–63 (1888).
- <sup>14</sup>J. Boussinesq, *Application des Potentiels à l'Étude de l'Équilibre et du Mouvement des Solides Élastiques* (Gauthier-Villars, 1885).
- <sup>15</sup>C. W. Oseen, *Neuere Methoden und Ergebnisse in der Hydrodynamik* (Akademische Verlagsgesellschaft M. B. H., 1927).
- <sup>16</sup>M. van Hinsberg, H. Clercx, and F. Toschi, "Enhanced settling of nonheavy inertial particles in homogeneous isotropic turbulence: The role of the pressure gradient and the Basset history force," *Phys. Rev. E* **95**, 023106 (2017).
- <sup>17</sup>H. K. Hassan and Y. A. Stepanyants, "Resonance properties of forced oscillations of particles and gaseous bubbles in a viscous fluid at small Reynolds numbers," *Phys. Fluids* **29**, 101703 (2017).
- <sup>18</sup>S. L. Seyler and S. Pressé, "Long-time persistence of hydrodynamic memory boosts microparticle transport," *Phys. Rev. Res.* **1**, 032003 (2019).
- <sup>19</sup>O. A. Druzhinin and L. A. Ostrovsky, "The influence of Basset force on particle dynamics in two-dimensional flows," *Physica D* **76**, 34–43 (1994).
- <sup>20</sup>F. Candelier, J. R. Angilella, and M. Souhar, "On the effect of the Boussinesq–Basset force on the radial migration of a Stokes particle in a vortex," *Phys. Fluids* **16**, 1765–1776 (2004).
- <sup>21</sup>A. Daitche, "On the role of the history force for inertial particles in turbulence," *J. Fluid Mech.* **782**, 567–593 (2015).
- <sup>22</sup>A. R. Premrata and H.-H. Wei, "The Basset problem with dynamic slip: Slip-induced memory effect and slip-stick transition," *J. Fluid Mech.* **866**, 431–449 (2019).
- <sup>23</sup>R. Gatignol, "On the history term of Boussinesq–Basset when the viscous fluid slips on the particle," *C. R. Mec.* **335**, 606–616 (2007).
- <sup>24</sup>I. Pienkowska, "Generalization of Faxen's theorems to include initial conditions," *Arch. Mech.* **33**, 469–480 (1981).
- <sup>25</sup>A. M. Albano, D. Bedeaux, and P. Mazur, "On the motion of a sphere with arbitrary slip in a viscous incompressible fluid," *Physica A* **80**, 89–97 (1975).
- <sup>26</sup>B. U. Felderhof, "Force density induced on a sphere in linear hydrodynamics," *Physica A* **84**, 569–576 (1976).
- <sup>27</sup>E. E. Michaelides and Z.-G. Feng, "The equation of motion of a small viscous sphere in an unsteady flow with interface slip," *Int. J. Multiphase Flow* **21**, 315–321 (1995).
- <sup>28</sup>E. A. Ashmawy, "Unsteady rotational motion of a slip spherical particle in a viscous fluid," *ISRN Math. Phys.* **2012**, 1–8.
- <sup>29</sup>A. R. Premrata and H.-H. Wei, "History hydrodynamic torque transitions in oscillatory spinning of stick-slip Janus particles," *AIP Adv.* **9**, 125113 (2019).
- <sup>30</sup>A. R. Premrata and H.-H. Wei, "Re-entrant history force transition for stick-slip Janus swimmers: Mixed Basset and slip-induced memory effects," *J. Fluid Mech.* **882**, A7 (2020).
- <sup>31</sup>S. M. Yang and L. G. Leal, "A note on memory-integral contributions to the force on an accelerating spherical drop at low Reynolds number," *Phys. Fluids A* **3**, 1822–1824 (1991).
- <sup>32</sup>V. Galindo and G. Gerbeth, "A note on the force on an accelerating spherical drop at low-Reynolds number," *Phys. Fluids A* **5**, 3290–3292 (1993).
- <sup>33</sup>J. K. Kabarowski and A. S. Khair, "Unsteady motion of a perfectly slipping sphere," *Phys. Rev. E* **101**, 053102 (2020).
- <sup>34</sup>L. H. Dill and R. Balasubramaniam, "Unsteady thermocapillary migration of isolated drops in creeping flow," *Int. J. Heat Fluid Flow* **13**, 78–85 (1992).
- <sup>35</sup>V. Sharanya and G. P. Raja Sekhar, "Thermocapillary migration of a spherical drop in an arbitrary transient Stokes flow," *Phys. Fluids* **27**, 063104 (2015).
- <sup>36</sup>R. Toegel, S. Luther, and D. Lohse, "Viscosity destabilizes sonoluminescing bubbles," *Phys. Rev. Lett.* **96**, 114301 (2006).
- <sup>37</sup>E. Igualada-Villodre, A. Medina-Palomo, P. Vega-Martínez, and J. Rodríguez-Rodríguez, "Transient effects in the translation of bubbles insonated with acoustic pulses of finite duration," *J. Fluid Mech.* **836**, 649–693 (2018).
- <sup>38</sup>R. Gorenflo, A. A. Kilbas, F. Mainardi, and S. V. Rogosin, *Mittag-Leffler Functions, Related Topics and Applications* (Springer, 2014).
- <sup>39</sup>R. F. Camargo, E. Capelas de Oliveira, and J. Vaz, Jr., "On anomalous diffusion and the fractional generalized Langevin equation for a harmonic oscillator," *J. Math. Phys.* **50**, 123518 (2009).
- <sup>40</sup>C. J. Lawrence and S. Weinbaum, "The force on an axisymmetric body in linearized, time-dependent motion: A new memory term," *J. Fluid Mech.* **171**, 209–218 (1986).

- <sup>41</sup>W. Zhang and H. A. Stone, "Oscillatory motions of circular disks and nearly spherical particles in viscous flows," *J. Fluid Mech.* **367**, 329–358 (1998).
- <sup>42</sup>H. Masoud and H. A. Stone, "The reciprocal theorem in fluid dynamics and transport phenomena," *J. Fluid Mech.* **879** (2019).
- <sup>43</sup>H. J. Keh and S. H. Chen, "The motion of a slip spherical particle in an arbitrary Stokes flow," *Eur. J. Mech., B: Fluids* **15**, 791–807 (1996).
- <sup>44</sup>G. K. Batchelor and J. T. Green, "The determination of the bulk stress in a suspension of spherical particles to order  $c^2$ ," *J. Fluid Mech.* **56**, 401–427 (1972).
- <sup>45</sup>S. B. Chen and X. Ye, "Faxen's laws of a composite sphere under creeping flow conditions," *J. Colloid Interface Sci.* **221**, 50–57 (2000).
- <sup>46</sup>J. W. Swan and A. S. Khair, "On the hydrodynamics of 'slip-stick'spheres," *J. Fluid Mech.* **606**, 115–132 (2008).
- <sup>47</sup>A. Ramachandran and A. S. Khair, "The dynamics and rheology of a dilute suspension of hydrodynamically Janus spheres in a linear flow," *J. Fluid Mech.* **633**, 233 (2009).
- <sup>48</sup>C. H. Hsiao and D. L. Young, "The singularity method in unsteady Stokes flow: Hydrodynamic force and torque around a sphere in time-dependent flows," *J. Fluid Mech.* **863**, 1–31 (2019).
- <sup>49</sup>H. Fujioka and H.-H. Wei, "Letter: New boundary layer structures due to strong wall slippage," *Phys. Fluids* **30**, 121702 (2018).
- <sup>50</sup>D. Legendre, A. Rachih, C. Souilliez, S. Charton, and E. Climent, "Basset-Boussinesq history force of a fluid sphere," *Phys. Rev. Fluids* **4**, 073603 (2019).
- <sup>51</sup>F. Feuillebois and A. Lasek, "On the rotational historic term in non-stationary Stokes flow," *Q. J. Mech. Appl. Math* **31**, 435–443 (1978).
- <sup>52</sup>C. Pozrikidis, "A singularity method for unsteady linearized flow," *Phys. Fluids A* **1**, 1508–1520 (1989).
- <sup>53</sup>U. Lei, C. Y. Yang, and K. C. Wu, "Viscous torque on a sphere under arbitrary rotation," *Appl. Phys. Lett.* **89**, 181908 (2006).
- <sup>54</sup>F. Candelier, J. Einarsson, and B. Mehlig, "Angular dynamics of a small particle in turbulence," *Phys. Rev. Lett.* **117**, 204501 (2016).
- <sup>55</sup>S. Kim and S. J. Karrila, *Microhydrodynamics: Principles and Selected Applications* (Butterworth-Heinemann, Boston, 1991).
- <sup>56</sup>R. Hocquart and E. J. Hinch, "The long-time tail of the angular-velocity autocorrelation function for a rigid Brownian particle of arbitrary centrally symmetric shape," *J. Fluid Mech.* **137**, 217–220 (1983).
- <sup>57</sup>A. Daitche and T. Tél, "Memory effects are relevant for chaotic advection of inertial particles," *Phys. Rev. Lett.* **107**, 244501 (2011).
- <sup>58</sup>A. Daitche and T. Tél, "Memory effects in chaotic advection of inertial particles," *New J. Phys.* **16**, 073008 (2014).